ACKNOWLEDGMENTS

I would like to thank my research advisor Dr. Douglas Crawford-Brown for his insight and guidance which has been invaluable to me in completing this project.

I would also like to thank Dr. Edward Chaney and Harris McMurry of the Radiation Oncology Department of North Carolina Memorial Hospital for their time and use of the resources of the Department.

A special thanks to my academic advisor Dr. James E. Watson who has helped to keep me on course throughout my graduate studies.

TABLE OF CONTENTS

LIST OF TABLES

Table

LIST OF FIGURES

Figure

ABSTRACT: A METHOD FOR UNFOLDING THE SPECTRUM OF NEUTRON ENERGIES PRODUCED BY MEDICAL LINEAR ACCELERATORS by William W. DeForest

The use of high energy linear accelerators for radiation therapy has given rise to an unexpected Health Physics concern. These accelerators are designed to produce electrons or photons in excess of 10 MeV. In recent years it has been noted that these accelerators are producing significant fluences of high energy neutrons which contribute greatly to the dose equivalent received by technicians and others in areas adjacent to treatment rooms. Proper shielding of these neutron fluences requires knowledge of the neutron spectrum at barriers to the treatment room. The present paper presents one method by which the neutron spectrum may be unfolded. The method makes use of Bonner Sphere data and matrix inversion computer codes to approximate the spectrum of neutrons produced by medical linear accelerators.

1. PURPOSE

The purpose of this research is to set forth a method by which a spectrum of neutron energies associated with neutrons produced by medical accelerators may be determined. A technique by which to unfold neutron spectra has been of great interest to the medical physics field since the advent of high energy linear accelerators used for radiation therapy.

These high energy linear accelerators are used to provide both electrons and, with the introduction of target materials, photons in excess of 20 MeV. Not long after these accelerators came into use, it became evident that neutrons were also being produced. Neutrons are produced primarily in the target and head shielding materials. These neutrons provide no medical benefit and can be thought of as contamination to the primary beam. A detrimental effect of the neutrons is to increase whole body dose to the patient. Technicians, and others in adjacent areas, may also be exposed to these neutrons due to their high penetrability and scattering characteristics. The whole body dose equivalent delivered to patients and others as a result of this contamination may be significant due to the high quality factors associated with neutrons.

Proper attenuation of neutron dose equivalents and fluences is not easy to achieve, even for monoenergetic beams. This is due to the fact that most interactions that neutrons go through produce secondary quanta that also must be

shielded. This picture is complicated in the use of medical accelerators because a spectrum of neutrons is produced. Because neutron reaction cross-sections change appreciably with neutron energy, the picture is still further complicated. Neutron spectra arise in accelerators due to the variety of neutron production modes and materials in which the neutrons are produced and interact.

Taking these points into consideration, it is evident that proper neutron shielding is difficult to predict. Furthermore, in order to make the attempt, knowledge of the neutron spectrum is a necessity.

This paper will investigate one method by which an approximation of a neutron spectrum may possibly be determined. The method makes use of Bonner sphere data, matrix inversion computer codes and smoothing routines to provide an estimate of the spectrum of neutron energies produced by a source. This method then is applied to measurements of neutron spectra produced by medical linear accelerators.

The research involved with developing this technique was carried out on a Siemens 20 linear accelerator located in the radiation therapy department at N.C. Memorial Hospital.

2. LITERATURE REVIEW

2a. Bonner Spheres Used in Previous Studies

The first use of a multisphere neutron spectrometer was presented by Bramblett, Ewing and Bonner[1] in 1960. In this

landmark paper, five polyethelyene spheres were used with diameters of 2, 3, 5, 8 and 12 inches. After this paper, these spheres became known as Bonner spheres. Bonner et al. used a Li(I) crystal scintillation detector located at the center of each sphere. The crystal size was kept to a minimum (4mm in dia. and 4mm thick) to provide good gamma discrimination. It was noted that 80% of incident thermal neutrons are absorbed in the 1st mm of the crystal, whereas a gamma deposits only a tiny fraction of it's energy in the entire volume of the crystal. By providing a large surface to volume ratio, the gamma discrimination effect is enhanced.

The purpose of the research by Bonner et al. was to determine the counting efficiency of each sphere as a function of neutron energy. In order to accomplish this, each of the spheres was exposed to a beam of monoenergetic neutrons of known fluence. Corrections were made for unequal illumination and background neutron counts. The curves that were generated were the basis for a large number of subsequent studies of neutron spectra, and also are used in this research. These curves are reproduced here in figure 1.

Li(I) detectors will count only those neutrons that are near thermal energies[1][2]. This is because large probabilities for neutron absorption in Li^6, given by the absorption cross section of Li^6, will only occur at these energies (see figure 2). The polyethylene spheres provide the function of slowing neutrons to thermal energies from their initial energies. The large H content of polyethylene absorbs

Figure .1.

Relative Counting Rate vs Energy for Moderating Spheres(1)

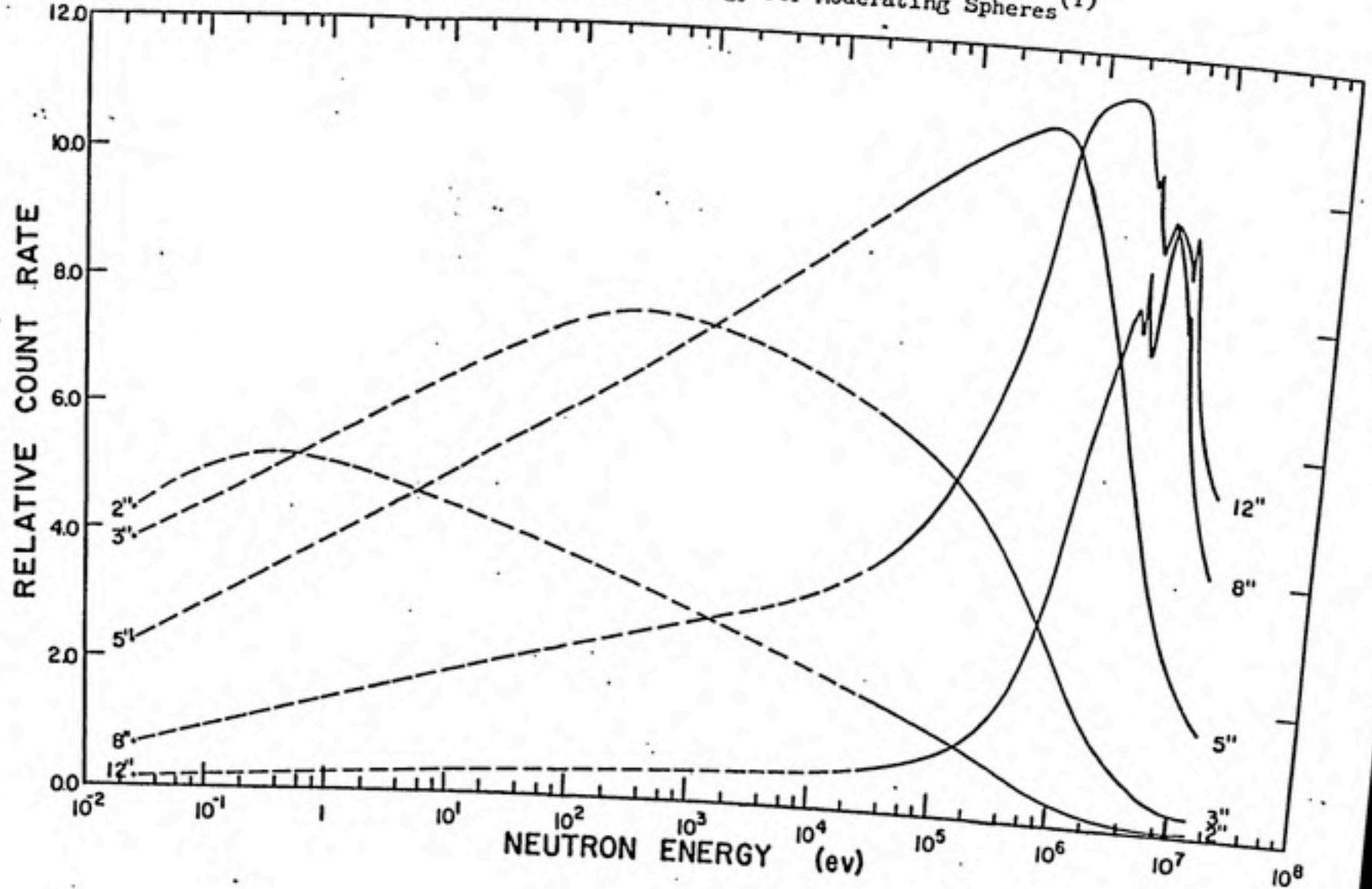

Figure 2.

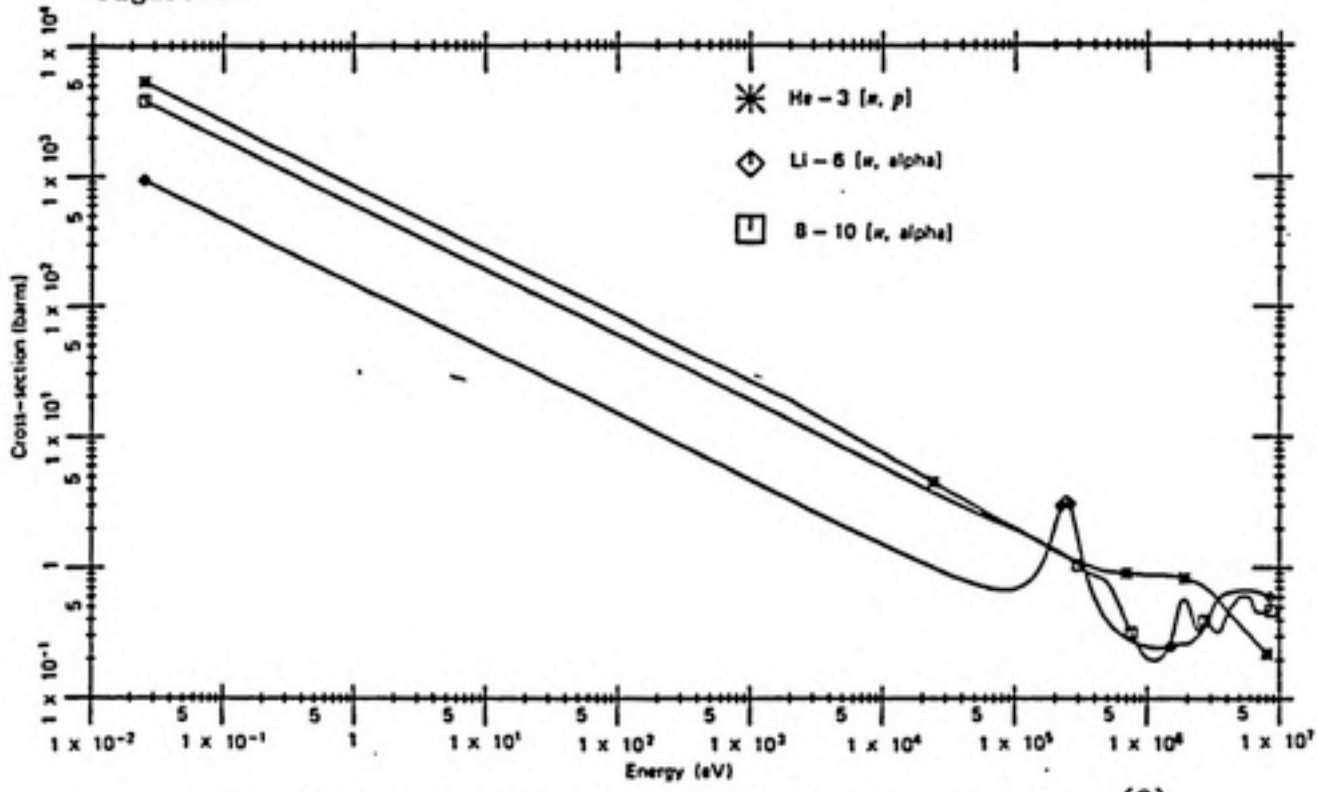

Cross section versus neutron energy for some reactions of interest in neutron detection.(2)

much of the energy of neutrons with each elastic collision with this light nucleus. For the bare and 3" diameter sphere size, Bonner et al. found that for neutron energies above 50 keV, count rates decreased with increases in energy. Larger spheres showed increases in count rates per unit fluence with increases in neutron energies, at least to a point. As energies were increased further, count rates per unit fluence dropped off quickly. In large spheres, neutrons with low energies prior to entering the sphere are captured before reaching the Li(I) crystal. Small spheres showed decreases in count rate per unit fluence with increases in neutron energy due to the fact that energetic neutrons were not slowed to thermal energies before reaching the Li(I) detector volume.

Bonner et al. suggested that further experiments to determine neutron energy distributions be performed with the source to detector distance as small as possible. This suggestion was intended to reduce the effects of background and to increase net counting rates.

Each sphere was placed over the detector and exposed to the neutron source. The number of interactions in the detector then was recorded for each sphere. This number was was equal to the sum of the number of interactions produced by neutrons in each energy interval considered by the researchers (the total neutron spectrum having previously been divided into discrete energy intervals).

The use of Bonner spheres then, yields a system of linear equations consisting of m equations and n unknowns. m is

given by the number of differently sized Bonner spheres used, while n is given by the number of neutron energy intervals to be solved for in characterizing the neutron energy spectrum.

Watkins and Holeman[3] suggest that data from Bonner spheres may be expressed as:

$$Y(i) = \int_{E_{min}}^{E_{max}} A(E,i)\ X(E)\ dE(i)$$

Here Y(i) is the count rate (counts/s) of the detector incorporating the ith size sphere, A(E,i) represents the response or counting efficiency (counts per N/cm^2) of the ith sphere for neutrons of energy E, and X(E) represents the actual intensity of the neutrons in the external neutron field and in a certain energy interval E to E + dE ($N/cm^2 s$). If the neutron spectrum is divided into a discrete number of energy intervals, the above equation also can be expressed as a linear matrix equation of the form

$$Y = AX \quad \text{(eq. 1)}$$

or equivalently

$$\begin{bmatrix} Y_1 \\ Y_2 \\ Y_3 \\ . \\ . \\ Y_m \end{bmatrix} = \begin{bmatrix} A_{1,1}, A_{1,2}, A_{1,3}, A_{1,4}, \cdots A_{1,n} \\ A_{1,2}, A_{2,2}, \cdots\cdots\cdots\cdots \\ A_{3,1} \\ . \\ . \\ A_{m,1}, A_{m,2}\cdots\cdots\cdots\cdots A_{mn} \end{bmatrix} \begin{bmatrix} X_1 \\ X_2 \\ X_3 \\ . \\ . \\ X_n \end{bmatrix} \quad \text{(eq. 2)}$$

In the matrix equation shown above (eq. 2), Y_1 through Y_m is the array of neutron count rates obtained from the separate

detector/Bonner sphere coverings exposed to a neutron source. A_{11} through A_{mn} is the matrix of response coefficients (counts/N/cm^2) for the detector/sphere combinations, with each row corresponding to a particular diameter of Bonner sphere for each of n energy intervals. In other words, A_{mn} is the response of the m^{th} detector/sphere combination to neutrons in the n^{th} energy interval. X is the array of neutron energy fluence values (N/cm^2), one for each of n neutron energy intervals. When the X values are multiplied by the corresponding A values and the products for each row are summed, a value of Y may be determined. This may be more easily understood in the following form.

$$Y_1 = A_{1,1}(X_1) + A_{1,2}(X_2) + A_{1,3}(X_3) + \ldots\ldots A_{1,n}\ (X_n)$$

Because the values of the A matrix are known from the literature, and the values of Y for any detector/sphere combination is known (determined by exposing detector/sphere combinations to the neutron source), the object is to invert the matrix equation and solve for the unknown elements of the X array. Solving for the X array gives the neutron fluence in each energy interval and hence the neutron spectrum.

Many techniques can be used to invert and solve a system of n linear equations and n unknowns, an example being through Gaussian elimination. Gaussian methods for solving n equations and n unknowns are well known. Using Bonner spheres, the maximum number of equations and unknowns would be seven, since seven spheres are commercially available. Although the Gaussian elimination method lends itself to

computer codes and would seem to simplify the problem of unfolding the spectrum (relative to use of the integral equation), it has drawbacks.

The first drawback is that only seven energy intervals would be generated for the spectrum. This causes many significant and important features to be omitted from the spectrum, such as the high energy (but low count rate) tail and narrow width energy peaks.

A second drawback of standard Gaussian techniques is that often negative results are obtained. This occurs in matrices of high singularity. Singularity refers to the condition often encountered in matrix equations where there is only one discrete solution array to the equation. This solution may be a very sensitive function of the values of Y_i. Small fluctuations in the values of Y (due to counting statistics), or small uncertainties in the values of A, may greatly influence the values of X that must be assumed in order to reproduce the values of the Y array. The Gaussian method obtains values of X without regard to the magnitude or sign of values in the X array. In order to solve the matrix equation for the unknown array, Gaussian methods may incorporate negative values into the solution array. In this case, these negative values would correspond to negative neutron fluence values for some neutron energy intervals, a situation which is physically impossible. The need therefore arose for an alternative iterative technique to be used, one which did not give any negative values to the solution array.

Rather than using a response matrix of 7 energy intervals, a larger number of neutron energy intervals in the response matrix would give much better energy resolution of the resulting neutron fluence array (X). Any number of response coefficients can be generated for detector/Bonner sphere combinations by determining the counting efficiency of each detector/sphere combination in monoenergetic neutron sources of known fluence. Conventional iterative techniques (such as Gaussian elimination) cannot be used in this case, however, due to the fact that there could be more unknowns than equations (i.e. n may exceed m). Fortunately there are other mathematical techniques, known as recursion methods, which yield an approximation of the array X when n exceeds m. These techniques start with an initial solution to X, which usually is obtained by multiplying the array Y by the inverse of the matrix A or by the identity matrix. The technique then slowly modifies X in a systematic manner (specific to the recursion method) until the product of A and X reproduces Y to a predetermined degree. At each point in the recursion, a check is made to ensure that all values of X cohere to certain restrictions such as physical plausibility (no negative values). The code then modifies the elements of X to yield a new solution, which is compared to the previous solution (and so on through a large number of iterations). An unfortunate problem with recursion routines is that the final solution for X often depends upon the choice of the initial solution. At the moment, however, recursion computer codes based on

modified iterative techniques seem to be the best choice for solving the resulting matrix of linear equations produced by Bonner sphere data in which n exceeds m. A methodology for such a technique was put forth in a paper by Watkins and Holeman[3]. Many authors have used a variety of techniques to unfold neutron spectra based on count rates obtained from Bonner Spheres. A 52 x 7 response matrix for A(E,i) has been computed by Hansen and Sandmier[4] containing response coefficients for 52 energy intervals and for 7 sizes of spherical polyethylene coverings. Watkins and Holeman[3] used a modified Scofield-Gold iterative technique, which approximates the unknown elements of a determined system of simultaneous equations using the diagonal elements of a diagonal matrix as the initial solution to X.

Various other iterative methods for solving equations similar to (1) and (2) have been summarized by Nachtigall and Burger[5] and Patterson and Thomas[5]. Lowery and Johnson[5] used a computer code based on the Scofield-Gold technique, known as SPUNIT, which was developed at Pacific Northwest Laboratories by Brackenbush and Scherpelz. This code gives non-negative solutions to the spectrum and smoothing of the spectrum could be added to the results. It is a technique such as this that has been used in the present research.

2b. Neutron Production

Modes of neutron production and data on neutron yields from electron linear accelerators have been discussed by many authors[7][8][9].

Neutrons are produced in the accelerator primarily when it is operated in the photon mode. In this mode, the photons are produced by introducing a target metal into the electron beam produced by the accelerator. Photons (X-rays) are produced as bremsstrahlung radiation in the target. These high energy photons then interact with the heavy nuclei shielding materials surrounding the accelerator head to produce fast neutrons.

The primary mode of production of neutrons is through the (γ,n) reaction with lesser contributions from the (γ,2n) and (γ,pn) reactions. Direct production of neutrons in either photon or electron modes is possible from the (e,n) and (e,e'n) reactions if the energy of the electron is sufficiently high. The production of neutrons from these electron reactions is smaller by a factor of over two orders of magnitude than the photoneutron reactions (due to the fine structure constant modified by several other factors). The production of neutrons from these electron reactions for the most part can be neglected [8].

For medical linear accelerators operating at less than 45 MeV, neutron production is largely due to reactions occurring in the giant photonuclear resonance, also known as the giant resonance. The cross section of this resonance is typified by a threshold, a rapid rise to a peak, and a gradual decrease of neutron production at the higher photon energies. For most of the medium to heavy nuclei shielding materials, the peak of the giant resonance occurs between 13 and 18 meV. The neutron

spectrum in the giant resonance has two major components. The first and largest component is the evaporation spectrum. In this component, neutrons are generated by compound nuclear formation. The nucleus may be thought of as being heated or excited by the photon, the result being that neutrons at the highest energy levels are "boiled out" of their potential well. The (ɣ,2n) separation energy occurs well within the giant resonance for most shielding materials and therefore contributes a significant number of neutrons to the total neutron fluence. One would think that protons, alphas, or other charged particles would be ejected from the nucleus from the absorption of a photon as well. This does not occur, however, because in the giant resonance sufficient energy is not imparted to charged particles (such as protons) to overcome the coulomb barrier for the elements of concern. The yield of photoneutrons may be thought of as being proportional to the convolution of the (ɣ,n) cross section and the bremsstrahlung spectrum [8].

The smaller component of the photonuclear giant resonance arises by the direct or photoionization process. In this process, one neutron acquires all of the photon's energy; the kinetic energy of the neutron then becomes equal to the photon's energy minus the binding energy of the neutron in the nucleus. The neutrons produced in this fashion are of much higher energy than those produced by the evaporation process. These neutrons then are responsible for the high energy tail on a photoneutron energy distribution plot (see fig 3). For

Figure 3.

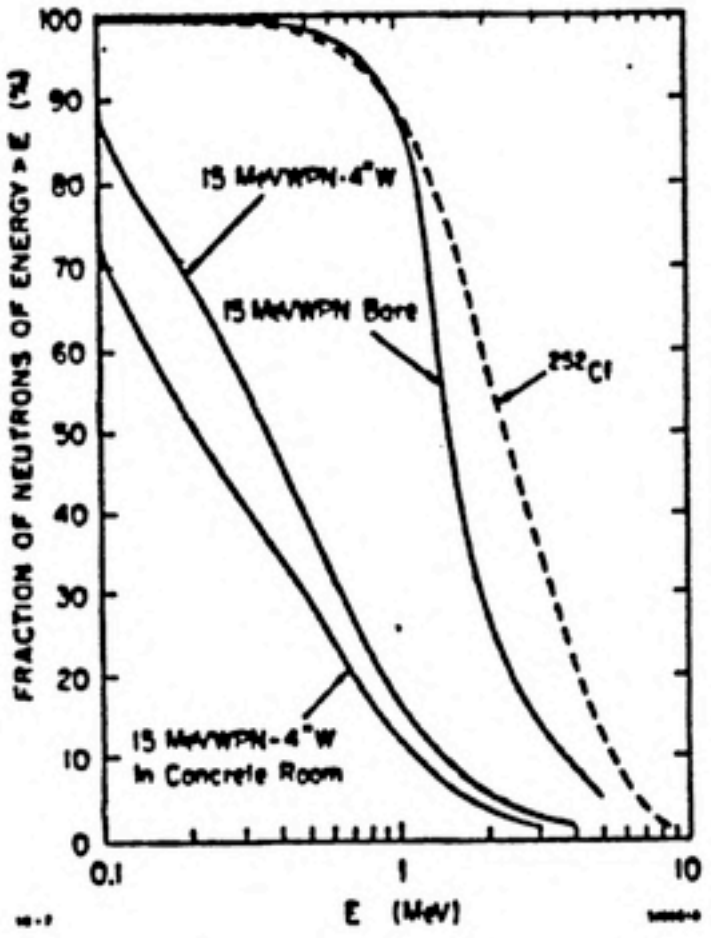

Various neutron integral spectra showing both accelerator primary spectrum and spectrum after passing through shielding. The Cf-252 spectrum is shown for comparison. Data are from the Monte-Carlo program MORSE[8].

this direct ejection of the neutron to occur, it is thought that the angular distribution for the emerging neutrons is slightly peaked at 90° to the incident photon [8][10].

Neutrons are produced inside the head of the accelerator and penetrate iostropically. Although the shielding incorporated into the head attenuates photons well, it does little to attenuate the fluence of neutrons. The only significant dose equivalent attenuation is from energy losses by the neutrons, this being due to inelastic scattering and (n,2n) reactions. This effectively reduces the energy and quality factor of the neutron.

Inelastic scattering occurs only at neutron energies above the lowest excited states of the shielding material; 0.6 - 0.8 MeV for lead, and 0.1 MeV for tungston. Obviously tungston is better for reducing the energy of neutrons. This reduction in energy provides a corresponding reduction in dose equivalent[10].

The (n,2n) reaction provides a minimal energy loss equal to the binding energy of the neutron in the nucleus. Unfortunately, it also provides two low energy neutrons of about equal energy that contribute greatly to the low energy neutron fluence in the treatment room [8][10].

After passing through a certain distance in any shielding material, essentially all the neutrons in the spectrum have had their energies reduced below the lowest excited state of the shielding materials. At these energies, inelastic scattering and the (n,2n) reaction can no longer occur.

Neutrons then may penetrate great distances through shielding materials in the head with no further energy loss or attenuation of dose equivalent.

The preceding discussion reviewed some of the factors that provide the source of neutrons in the treatment room. The intensity of neutrons from this source as a function of the distance from the accelerator head can be described by the inverse square law. There is, however, a second component comprised of thermal neutrons which have scattered inelasticly (and elasticly) off the inside walls of the treatment room. The fluence of these low energy neutrons is essentially constant throughout the room. This thermal neutron fluence is related to the fast neutron fluence by

$$\phi = K(Q/S)$$

where: ϕ is the thermal neutron fluence, Q is the fast neutron fluence, S is the inside surface area of the treatment room and K is a constant related to the type of shielding used in the head of the accelerator [11].

It has been found that photons are always more penetrating than neutrons for the energy ranges of interest in a medical accelerator. While producing photons of 20 MeV, the average energy of the neutron spectrum emerging from the accelerator head is never much above 1 MeV. If a therapy room is constructed of enough concrete to sufficiently attenuate the photons produced, the neutrons will also be modified and captured by the large hydrogen content of the concrete. The problem in neutron shielding, then, is found at the maze

doorways and any other penetrations to the room, (ducts, conduits, etc.). In these areas, neutrons may easily scatter to areas unprotected by the massive concrete walls [10].

3. THEORY OF NEUTRON MEASUREMENT WITH BONNER SPHERES

Currently, methods used to calculate neutron shielding for therapy rooms have been rules of thumb and educated guesses. Little is known about the spectrum of neutron energies given off by accelerators or how this spectrum changes as the neutrons pass through various shielding materials. Exact methods for determining required neutron shielding, therefore, are available but rarely used. It is extremely important that barriers be devised to absorb neutrons and/or reflect neutrons back to the treatment room.

It is necessary to know the spectrum of neutron energies in order to properly determine the nature of shielding needed. It is equally important to know how the spectrum changes as neutrons pass through shields of various constructions. In this way it will be possible to develop a series of equations to take the guess work out of neutron shielding for medical linear accelerator facilities.

In order to determine neutron spectra, a series of different sized Bonner spheres are often used. Although most researchers have used Bonner spheres to moderate the neutrons, many types of detectors, placed at the center of the sphere to detect the moderated neutrons, can be used. A Li(I)

scintillation detector, which is a thermal neutron detector, is a good choice. Upon absorption of the neutron, the $Li^6(n,\alpha)H^3$ reaction takes place, releasing an alpha particle. The track length of the alpha is sufficiently short to deposit all of it's energy in the crystal. The amount of energy released in the crystal will be in the neighborhood of 4.7 MeV and will be the same for each neutron absorbed. This release of energy results in a pulse. The electrical pulses from the Li(I) detector located at the center of each sphere then would all be of the same height regardless of the energy of the interacting neutron. The only information gained from each of the detectors therefore is a count rate. As Li(I) scintillation detectors will also record photons interacting in the crystal, a means of discriminating between neutrons and photons must be addressed. This is particularly important since most neutron fields are accompanied by an appreciable field of photons. The small (4mm x 4mm) size of the Li(I) crystal helps in this respect. Photons, with their low LETs, will deposit only a tiny fraction of their energy in the detector. This will result in a very small pulse size compared with the neutron pulse size. By properly setting counting thresholds, or by using similar methods, it is possible to successfully count only the neutron pulses and discriminate against pulses produced by photons. Problems arise only when high photon fluences yield significant pile up.

Bonner spheres provide the function of thermalizing fast neutrons. Neutrons that are sufficiently thermalized by the sphere, but not absorbed in the sphere, then will be absorbed in the Li(I) crystal according to the intrinsic detection efficiency of the crystal at that neutron energy.

4. MATERIALS AND METHODS

4a. Neutron Counting Equipment

A series of four Bonner spheres manufactured by Ludlum was used in this research to establish neutron spectra. The sizes of the spheres were: 3", 5", 8", and 12" in diameter. A bare detector was also used as one of the detector/sphere combinations. The Li(I) crystal, light pipe, and PM assembly were also obtained from Ludlum.

A coaxial cable, designed to carry both the signal and the high voltage for the detector, was connected to the PM tube with a type C connector. The other end of the coaxial cable was hooked to a Ludlum signal splitter, designed to split the high voltage and the signal. High voltage was supplied to the splitter and hence the PM tube by a separate HV supply (manufactured by Power Designs). Leaving the splitter, the signal travels via coaxial cable to an Ortec pre amp set on 500 pF. The pre amp was hooked via coaxial cable to an Ortec amplifier set on a gain of 20. Output of the amp was then hooked up to a Northern Multi Channel Analyzer (MCA). The HV supply, amp, and pre amp were contained in a portable N.I.M. bin for easy transport (see figure 4). An MCA was

chosen in preference to a scaler to aid in discrimination between neutron and photon pulses. Typically, photon discrimination is a difficult task with Li(I) crystals (used for neutron measurements) since it involves minute adjustment and readjustment of sensitive discriminator and threshold settings. Discrimination of photon counts from neutron counts is easily accomplished visually with the MCA. The low photon detection efficiency of the Li(I) crystal results in a low, prominent compton shoulder seen on the MCA. The neutron counts, however, are at much higher channel numbers due to nearly complete energy absorption of the secondary alpha. The neutron counts also form a prominent peak, so total neutron counts are easily obtained by integrating under this peak by setting regions of interest on the MCA or by plotting the peaks and integrating by hand.

It was decided that the component system and it's ability to deliver neutron counts needed to be tested. The detector/sphere combinations were exposed to a uniform field of neutrons (and photons) emanating from a PuBe source located at the Physics Department at UNC. Each sphere was exposed to the PuBe source for 10 minutes and counts were obtained. The data obtained were interpreted by setting up a matrix similar to eq. 2 and solving using a computer program described in the next sub-section. This test was initially intended only as a test of the neutron counting system. It was later decided to use the data obtained as input to the computer program

Figure 4

Diagram of neutron counting system

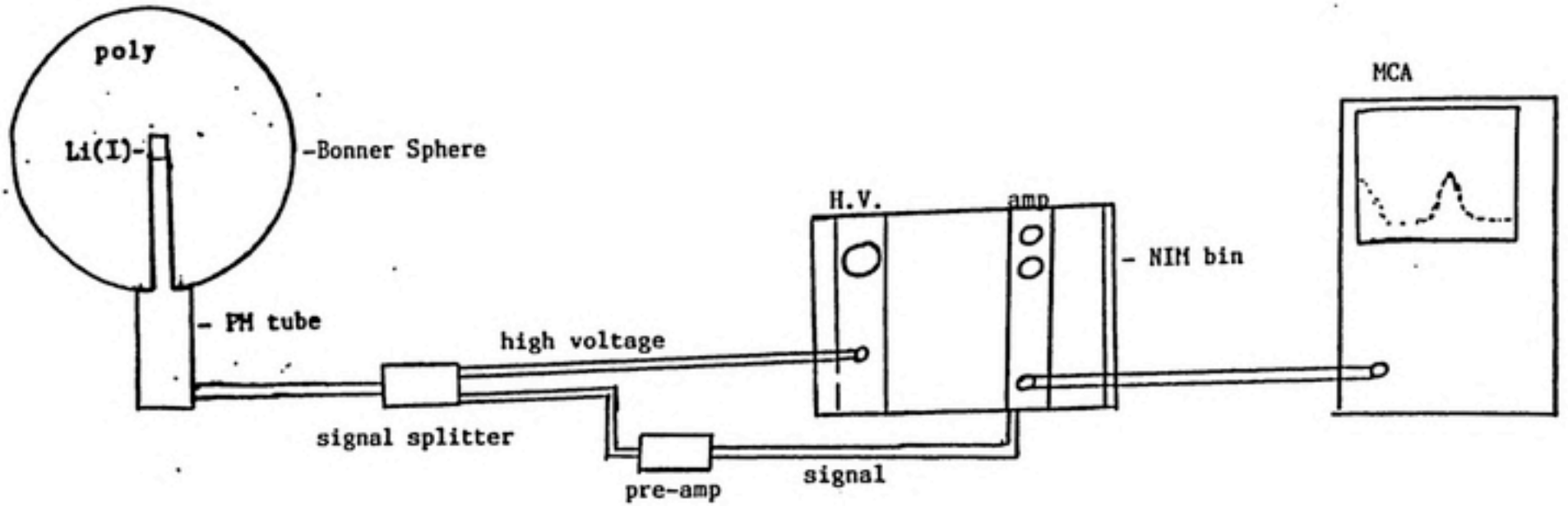

described in 4b. as a test of the code's ability to solve matrix equations of various sizes.

The neutron counting system was taken to the Radiation Therapy department at N.C. Memorial Hospital and set up in the therapy room containing the Siemens 20 linear accelerator. The configuration and position of the equipment is shown in figure 5. The detector/sphere setup was placed approximately 1.3 meters off the floor directly between the head and the door to the maze at approximately 2 meters from the head. The accelerator was set to deliver 18 MeV photons. Each detector/sphere combination was exposed to photons and neutrons resulting from identical runs on the accelerator delivering 400 rads to an imaginary patient. No phantom material was added to intercept the beam as this would only serve to increase photon scatter and potentially decrease neutron fluences through elastic scattering and radiative capture in hydrogen.

Pulse height spectra were obtained for each accelerator run. Neutron counts for each detector/sphere combination were determined through integrating the neutron pulse height spectrum by hand. This was done because the photon continuum was of much greater energy and height than is normally encountered in neutron spectroscopy due to photon pile-up, and assumptions had to be made as to the shapes of some of the neutron peaks in order to correctly subtract off photon counts. The neutron peak was sitting on top of the high energy side of the photon peak. In order to subtract off

Figure 5.

Diagram of radiation therapy treatment room at N.C. Memorial Hospital containing linear accelerator showing position of Bonner Sphere detectors.

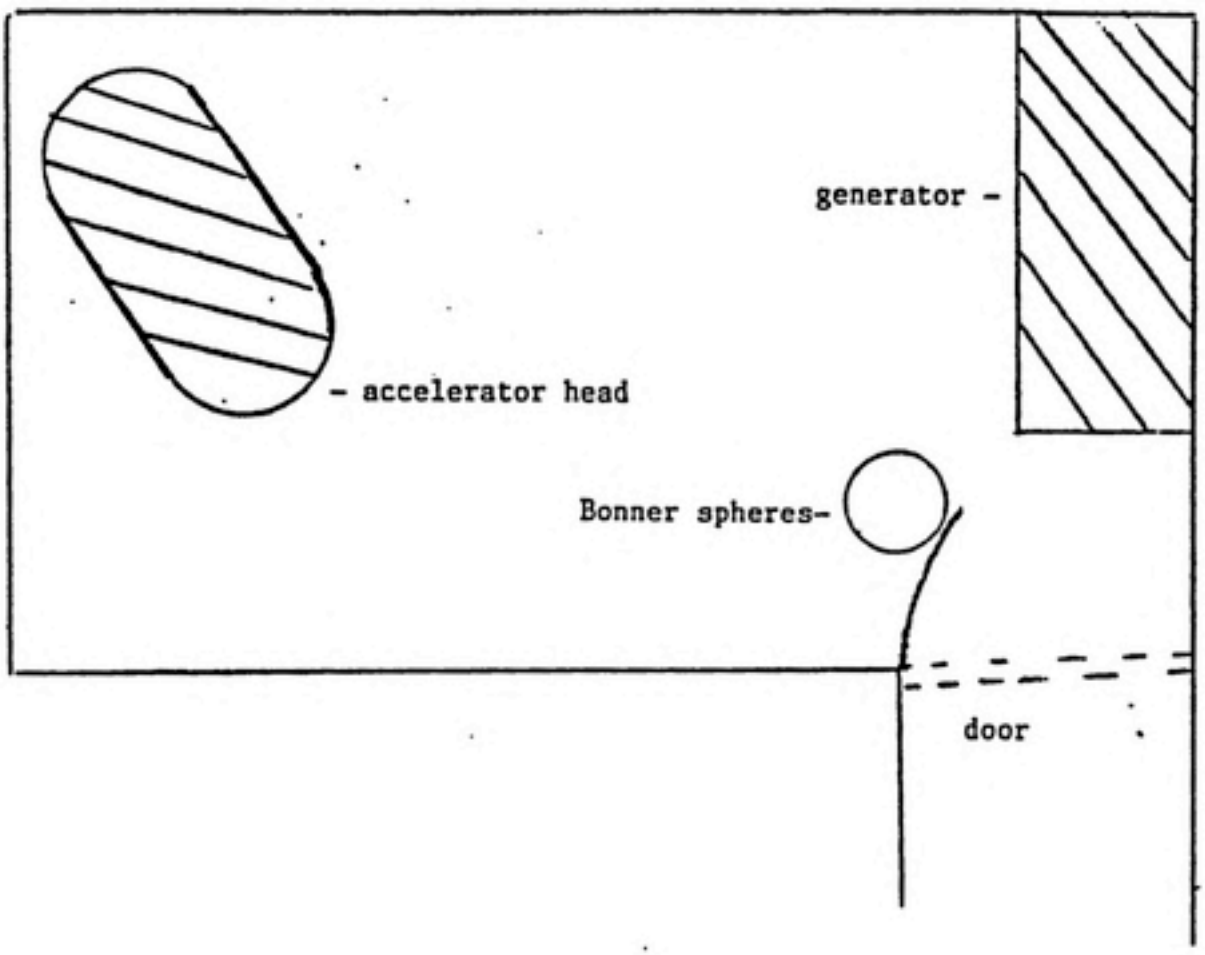

photon counts, the high energy slope of the photon peak was assumed to be exponential in nature, and photon counts were subtracted off using valley to valley averaging.

4b. The Computer Program

The data obtained from the PuBe source were at first evaluated using standard matrix inversion (Gaussian elimination method). Using this method, negative fluences were obtained in some of the 5 energy intervals. It was summized that a possible reason for these results was the highly singular nature of the matrix equation. It was also noted that the response curves for the 8" and 10" spheres were extremely similar in nature (fig. 1). That is to say, the curves were linearly dependent (i.e. theresponse varied with energy at approximately the same rate). When solving matrix equations, linear dependence between two equations heightens problems encountered with singularity and thereby increases the probability of obtaining negative results. In an attempt to solve future problems of singularity, it was decided that the 10" sphere would not be used and the bare detector would be used as the fifth detector/covering combination (at this time computer codes based on Gaussian elimination methods were still being used in this research).

In order to resolve the problem of negative fluences, and to obtain a more detailed neutron spectrum, a recursion approach in which n exceeded m was adopted. Available data in the response matrix, A, included estimates of the response in 52 neutron energy intervals for each sphere diameter[4] (see

table 1).

The unknown element in the system of linear equations to solve for is the neutron fluence (X) in each of the 52 energy intervals. As mentioned before, conventional computer codes which solve for the unknown elements by inversion cannot be used in this case since the number of unknowns is larger than the number of equations.

There was a necessity, then, for a computer code to be written based on the Scofield-Gold iterative technique. The Scofield-Gold iterative technique basically operates like other iterative techniques in that it successively alters (in some consistent manner) the elements of the solution array (in this case X) until closest agreement between Y and the product of A and X is found. The computed solution array (X) then is at best a possible close approximation of the true solution array, with other approximate solutions being possible. It is possible to determine in a quantitative manner how close to the true solution array (X_T) the computed approximation (X_C) is by calculating the difference between Y and the product of A and X_C. An additional computer code was written to calculate this difference with each iteration. The computer code written for the present research replaces the computed values of the solution array (in this case the approximated neutron spectrum X_C) back into the matrix equation (equation 2) and computes the left hand side of the matrix equation (see equation 2). This new calculated product is labelled as the vector array P in the computer code (P referring to the

Table 1. 52 x 5 response matrix for Bonner Spheres

interval	N energy (eV)	Bare	3" sphere	5" sphere	8" sphere	12" sphere
1	1.0E-2	0.1220	0.1059	0.0540	0.0156	0.0024
2	1.6E-2	0.1220	0.1087	0.0560	0.0162	0.0025
3	2.5E-2	0.1220	0.1140	0.0588	0.0171	0.0026
4	4.0E-2	0.1180	0.1225	0.0639	0.0185	0.0029
5	6.3E-2	0.1160	0.1446	0.0712	0.0207	0.0032
6	1.0E-1	0.1140	0.1530	0.0824	0.0240	0.0037
7	1.6E-1	0.1100	0.1787	0.0975	0.0285	0.0044
8	2.5E-1	0.1020	0.2050	0.1141	0.0333	0.0051
9	4.0E-1	0.1160	0.2326	0.1327	0.0386	0.0059
10	6.3E-1	0.1100	0.2560	0.1480	0.0433	0.0065
11	1.0	0.0840	0.2701	0.1605	0.0479	0.0071
12	1.6	0.0760	0.2809	0.1710	0.0517	0.0080
13	2.5	0.0680	0.2853	0.1818	0.0541	0.0082
14	4.0	0.0600	0.2872	0.1897	0.0572	0.0088
15	6.3	0.0520	0.2880	0.1971	0.0598	0.0091
16	1.0E1	0.0420	0.2877	0.2033	0.0617	0.0096
17	1.6E1	0.0360	0.2847	0.2094	0.0647	0.0100
18	2.5E1	0.0280	0.2800	0.2150	0.0675	0.0105
19	4.0E1	0.0200	0.2743	0.2203	0.0707	0.0111
20	6.3E1	0.0100	0.2672	0.2252	0.0732	0.0113
21	1.0E2	0.0020	0.2608	0.2292	0.0763	0.0117
22	1.6E2	0.0000	0.2535	0.2236	0.0789	0.0122
23	2.5E2	0.0000	0.2451	0.2349	0.0816	0.0127
24	4.0E2	0.0000	0.2362	0.2357	0.0829	0.0129
25	6.3E2	0.0000	0.2227	0.2363	0.0842.	0.0130
26	1.0E3	0.0000	0.2187	0.2375	0.0865	0.0132
27	1.6E3	0.0000	0.2107	0.2392	0.0901	0.0142
28	2.5E3	0.0000	0.2050	0.2409	0.0935	0.0150
29	4.0E3	0.0000	0.1915	0.2412	0.0956	0.0153
30	6.3E3	0.0000	0.1850	0.2418	0.0983	0.0158
31	1.0E4	0.0000	0.1780	0.2423	0.1023	0.0167
32	1.6E4	0.0000	0.1707	0.2445	0.1069	0.0171
33	2.5E4	0.0000	0.1625	0.2453	0.1106	0.0181
34	4.0E4	0.0000	0.1532	0.2474	0.1178	0.0197
35	6.3E4	0.0000	0.1457	0.2499	0.1266	0.0220
36	1.0E5	0.0000	0.1372	0.2536	0.1402	0.0256
37	1.6E5	0.0000	0.1258	0.2591	0.1582	0.0312
38	2.5E5	0.0000	0.1120	0.2644	0.1792	0.0396
39	4.0E5	0.0000	0.0950	0.2641	0.2063	0.0533
40	6.3E5	0.0000	0.0788	0.2520	0.2356	0.0745
41	1.0E6	0.0000	0.0600	0.2310	0.2705	0.1040
42	1.6E6	0.0000	0.0390	0.2050	0.2720	0.1500
43	2.5E6	0.0000	0.0287	0.1550	0.2640	0.1856
44	4.0E6	0.0000	0.0191	0.1153	0.2380	0.2067
45	6.3E6	0.0000	0.0130	0.0685	0.1950	0.1995
46	1.7E7	0.0000	0.0074	0.0563	0.1415	0.1742
47	1.6E7	0.0000	0.0041	0.0337	0.0992	0.1420
48	2.5E7	0.0000	0.0020	0.0205	0.0737	0.1141
49	4.0E7	0.0000	0.0010	0.0130	0.0476	0.0853
50	6.3E7	0.0000	0.0004	0.0056	0.0265	0.0543
51	1.0E8	0.0000	0.0003	0.0037	0.0152	0.0266
52	1.6E8	0.0000	0.0001	0.0001	0.0035	0.0150

predicted counts). The squared difference between the newly computed left hand side (P) of the matrix equation and the actual left hand side of the matrix equation (in this case the measurements Y) is taken as the residual. This calculation is performed for each of the 5 equations and the residuals summed after each iteration. The computed solution array with the lowest summed residual would be the best approximation of the solution array, or the "best fit".

The iterative technique must have some initial solution array (X) from which to start. This initial array could be provided, based on educated guesses about the neutron spectrum, as input, could be calculated by the computer program using the product of Y and the inverse of A, or could be obtained by multiplying Y by the identity matrix. It was decided to take the latter course since there was no information on which to base an initial guess about the neutron spectrum.

In summary, then, the recursion code used in the present study begins with an initial approximation to the neutron spectrum. This approximation is obtained by multiplying the Y array (i.e. the data array) by a diagonal matrix, D. In the initial step of the recursion, X is set equal to the product of Y and D, then is multiplied by A and the product compared to Y (i.e. the residual is computed). The elements of D then are adjusted by the recursion routine to new values, and a new solution to X is obtained. These adjustments occur by systematically exploring the effect of small changes in each

element of the previous solution array (X), with the change producing the largest decrease in residual being selected at each point of the iteration. This process continues through a large number of iterations (1500), with the elements of D changing with each iteration. The result is a total of 1500 approximations to X, each with an associated residual. Log-log smoothing also is added to each approximation of the X matrix before the residual is computed. This smoothing simply causes the histogram of X (which contains 52 energy intervals) to become less subject to large changes in the number of neutrons in adjacent energy intervals. Log-log smoothing is included to preclude the development of a wildly fluctuating curve. A more or less smooth neutron spectrum is expected. Log-log smoothing is applied during each loop of the recursion routine to each element of the X array, X(n), as well as to X(n+1) and X(n-1). This serves to take erratic jumps out of the curve and give a potentially more reasonable spectrum. The program was written to continue through 1500 successive approximations of the X matrix (lines 41 through 118 of the computer program in appx. A).

Each time through this iteration the program takes the current value of each element of the fluence array X and multiplies it by the corresponding response coefficient (from matrix A) in a given energy interval for each detector sphere/combination. Summing these products together for each detector/sphere combination, an array analogous to the experimentally determined neutron count array Y is developed.

The elements of this predicted count array are placed into an array named P (lines 85 - 91 of the computer program in appx. A)

The value of the elements of the P array, when compared to the value of the elements of the Y array, provides a test as to how closely the solution array (X_C) is able to reproduce the elements of the Y array. A residual array may then be computed from the squared difference between the elements of the P and Y arrays for each detector/sphere combination. This residual array is labeled array R in the program code (lines 92 and 93 of the computer program in appx. A). The total residual for each loop of the recursion routine may then be determined as the sum of the elements of the R array (one value for each detector/sphere combination). These total residuals for each loop are stored as elements of array AL, a vector array of 1500 elements (one for each loop of the recursion routine). From the information in this array, the step which contains the best approximation of the X matrix could be determined by searching for the lowest residual.

There is much debate in the physics community as to which recursion routine, if any, is best for solving matrix equations for neutron spectra. For this reason it was decided that in addition to running the iterative-smoothing routine (which includes both recursion and smoothing), both the iterative and smoothing routines alone would be applied independently to the data. This led to the development of three different versions of the computer program, each of

which was applied to both sets of data (the PuBe and accelerator data). The iterative routine alone is able to solve the matrix equation (2) for the values of X although discontinuities in the spectrum might result. It was felt that the log-log smoothing routine alone might also approximate the solution to the matrix equation. The smoothing routine could accomplish this by successively smoothing the initial spectrum as produced in lines 19 through 40 of the computer program (appx. A), although the final shape of the spectrum would be heavily influenced by the kind of smoothing employed. It was also not clear whether the use of smoothing alone would allow convergence onto a solution in an efficient manner or would lead to a physically realistic solution spectrum (i.e. the elements of the X array).

5. RESULTS

Total counts within the neutron peak for each of the five detector/sphere combinations exposed to the PuBe source are outlined in table 2 (integration by the MCA). The reader should note that the data from the 10" sphere as well as the bare detector are omitted. This is because no data were gathered for the bare detector, since problems with the linear dependence of the 8" and 10" spheres data had not yet been noted during the course of the research.

The total neutron counts under the peak for each of the detector/sphere combinations exposed to the accelerator follow in table 3 (Integration was performed by hand using valley-to-

TABLE 2
PuBe source data, 10 min. counting time for each detector/sphere combination.

Poly sphere covering	Counts
3"	642
5"	1088
8"	1497
12"	1214

TABLE 3
Accelerator data, 400 rads delivered to each detector/sphere, counting times equal.

Poly sphere covering	Counts
Bare	5,875
3"	63,000
5"	42,725
8"	7,900
12"	675

valley averaging).

Both sets of data then were input into each of the three forms of the program (smoothing alone, iteration alone, iteration plus smoothing) as elements of the Y matrix. Through analysis of the residual array output data for computer runs made on the PuBe source data it was determined that the best approximation of the X (neutron fluence) matrix was to be found at step 580 of the recursion loop for the log-log smoothing only routine, and at step 1500 for the iteration only and iteration-smoothing routines. For runs of the computer programs utilizing the accelerator data it was found that the best approximation of the fluence matrix was to be found at step 875 of the recursion loop for the smoothing only routine, step 1500 for the iteration only trial, and step 338 for the iteration-smoothing trial. The X matrix was plotted at each of these steps. Spectra were printed at additional steps to gain an understanding as to how the recursion routines successively approximated the X matrix. The reader should see figures 6 thru 11 for plots of these X matrices (neutron spectra). The program also output the value for the P (predicted Bonner sphere counts) array at all "Best Fit" steps (tables 4, 5, 6, 7, 8, 9) to determine how well the X array is able to reproduce the Y array by visually comparing the P array to the Y array.

The reader may refer to tables 4 through 9 for data on observed counts, predicted counts, standard deviation of counts and percent deviation ([observed-predicted]/observed)

Figure 6.

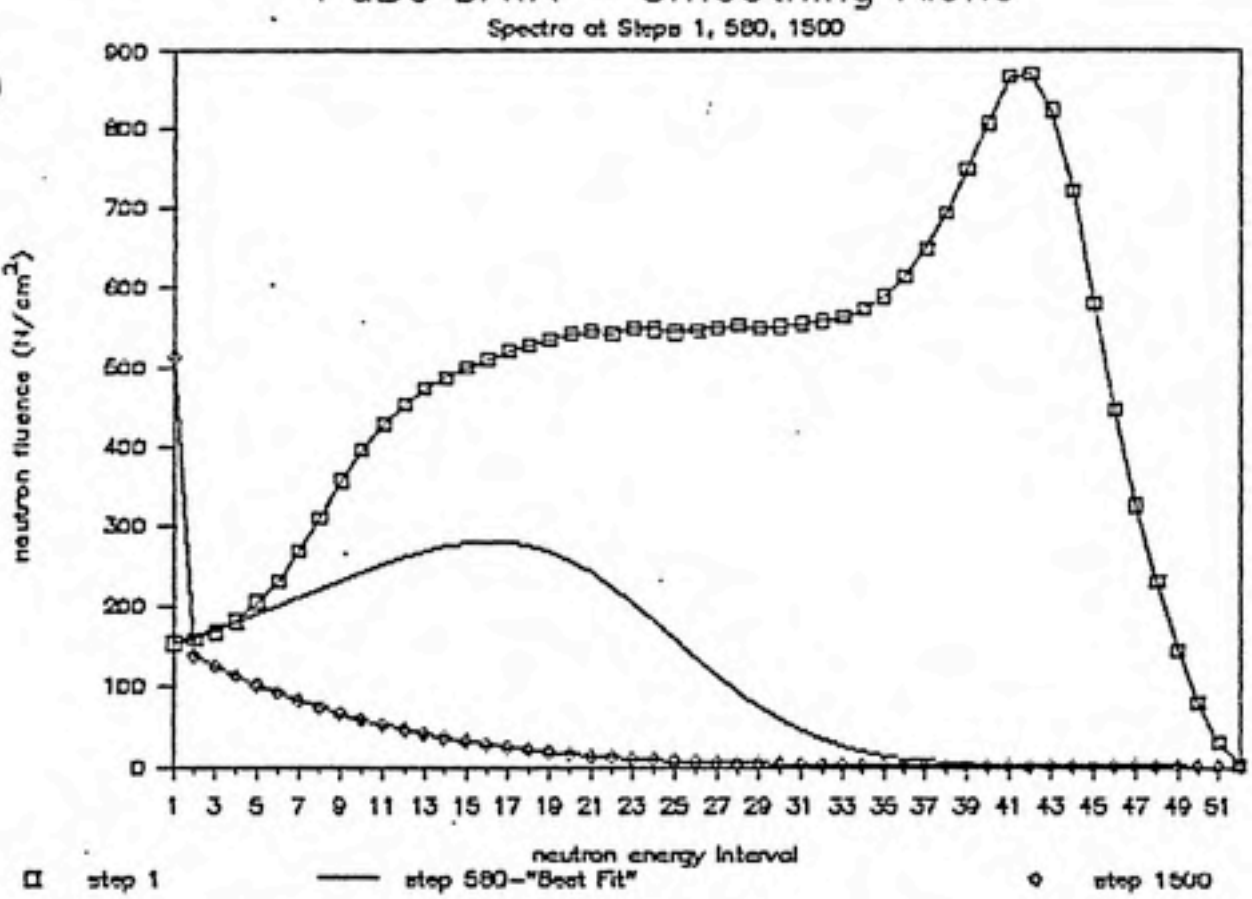

Figure 7.

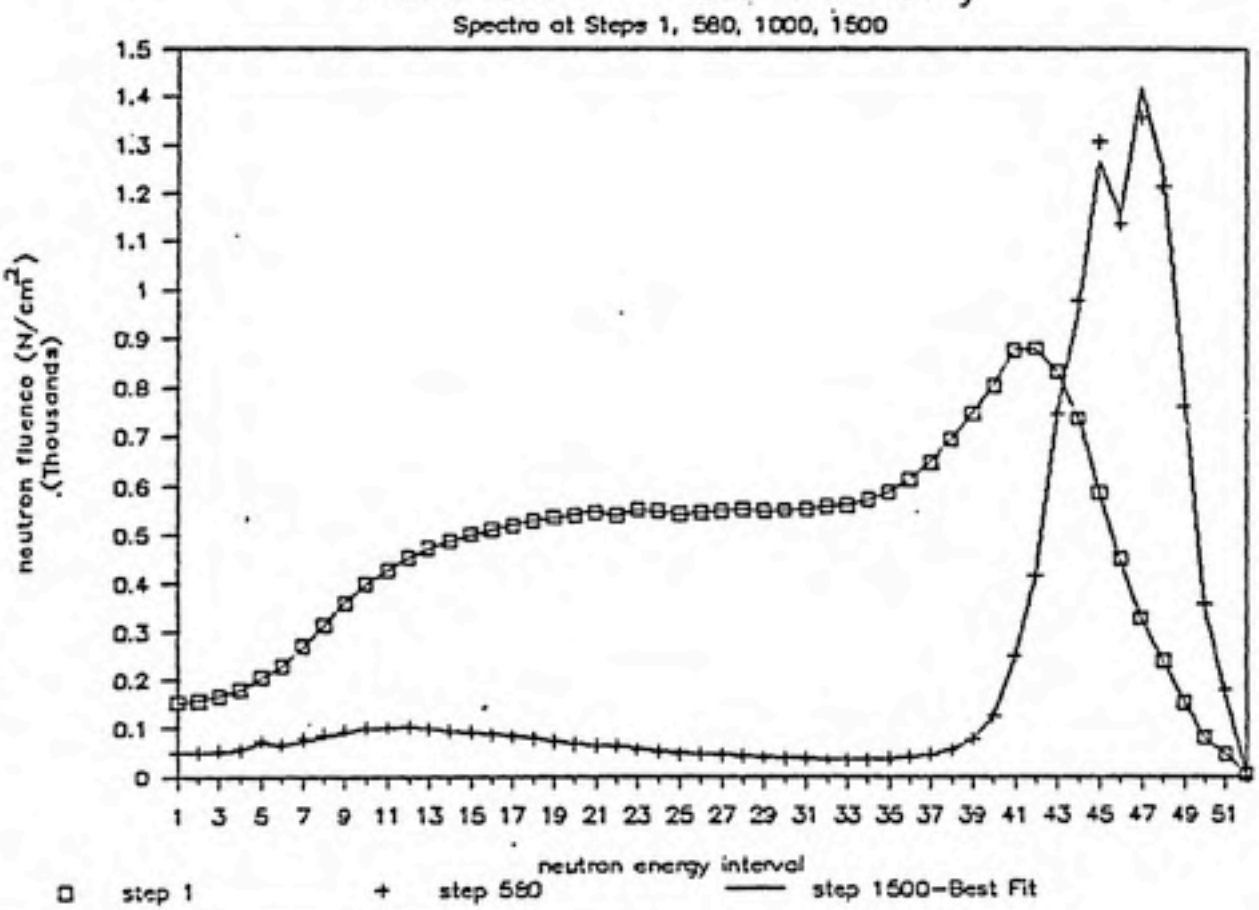

Figure 8.

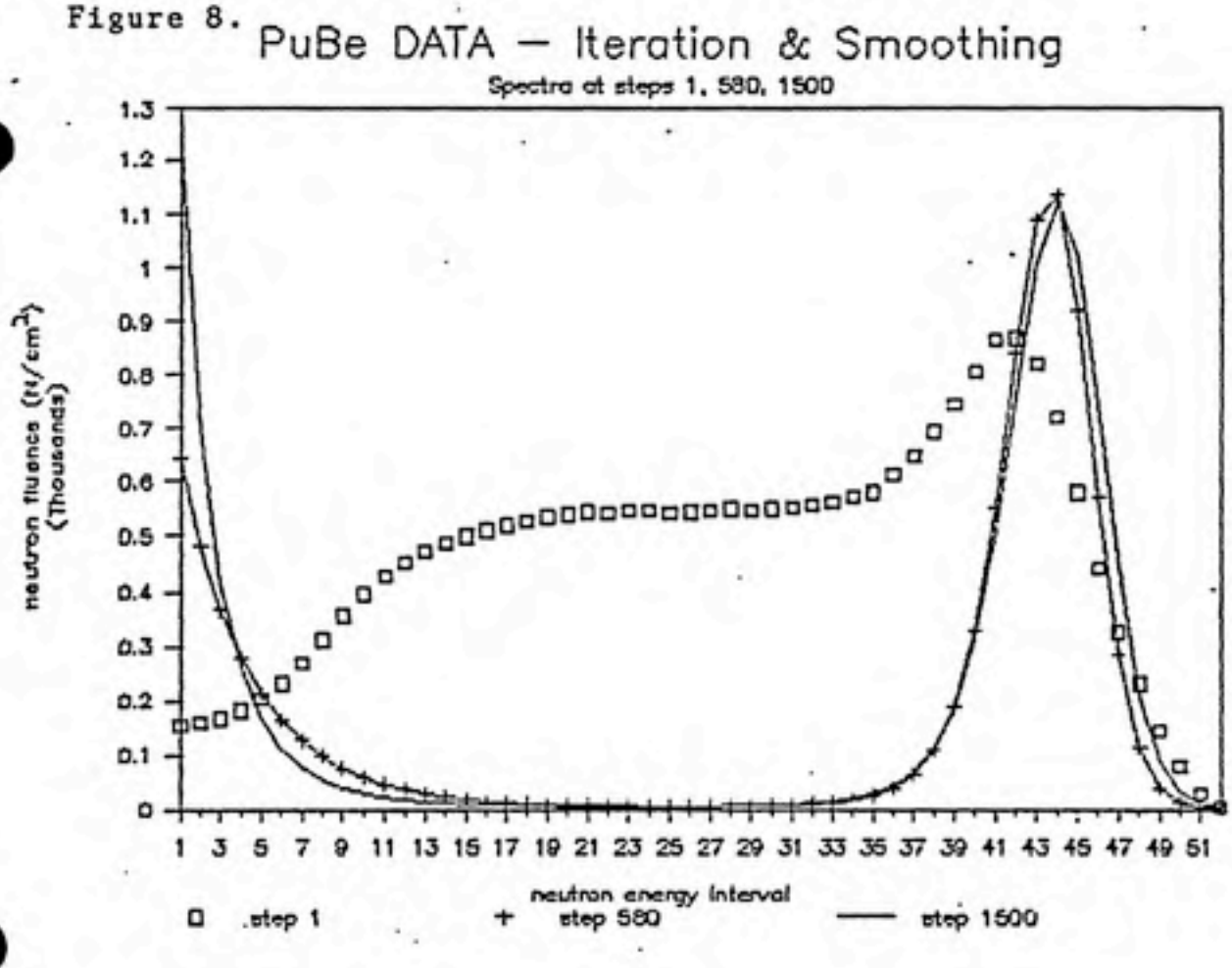

Figure 9.

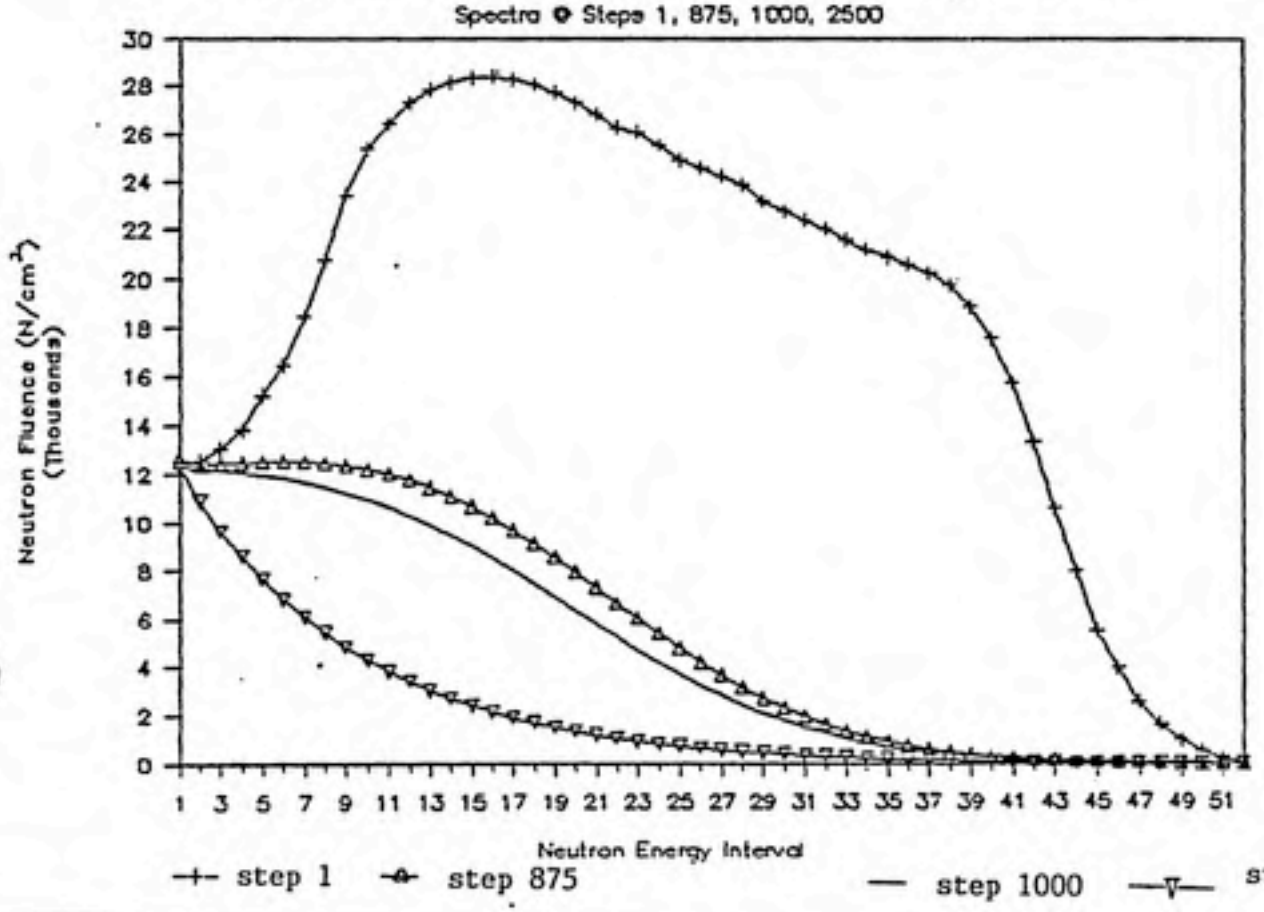

Figure 10.

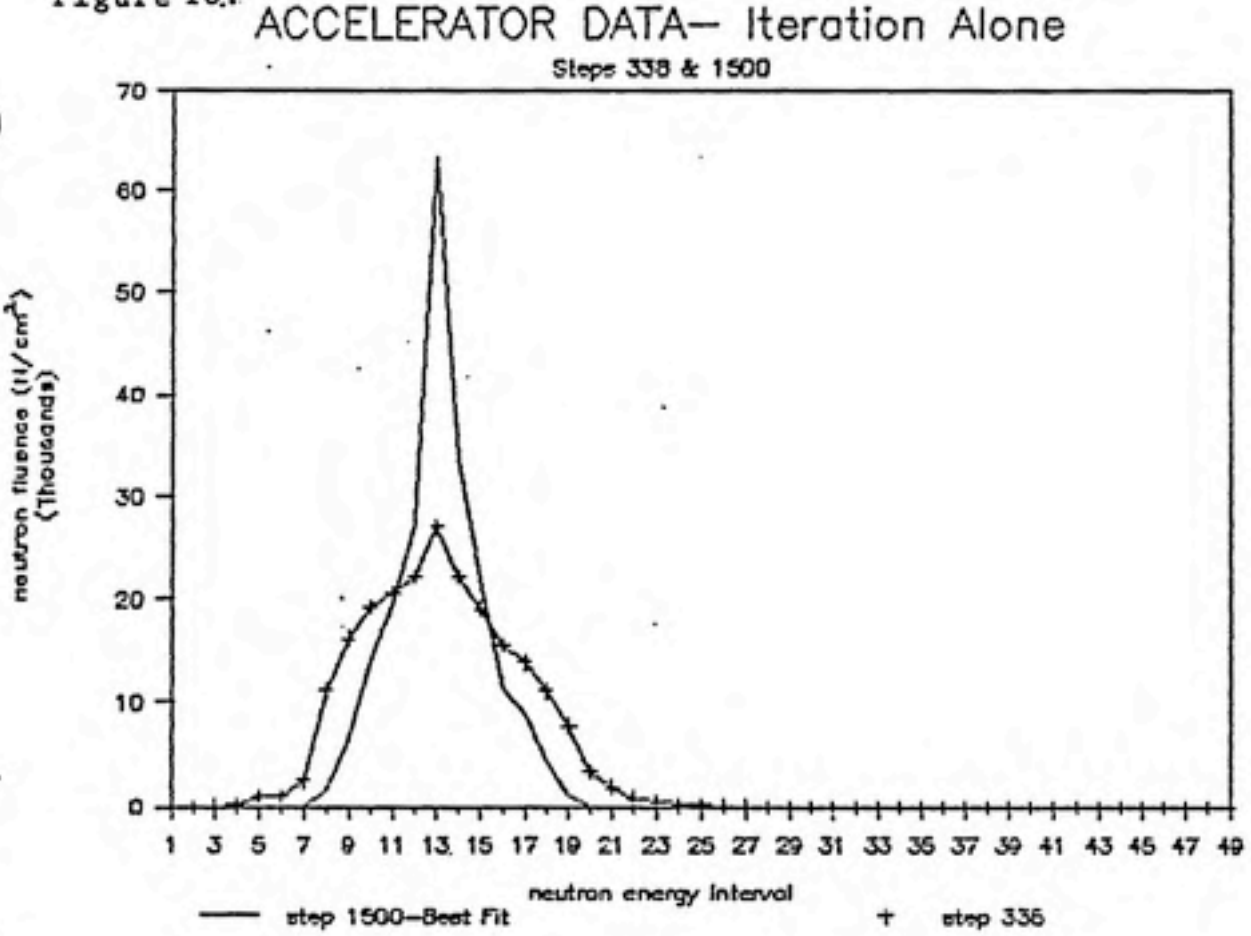

Figure 11.

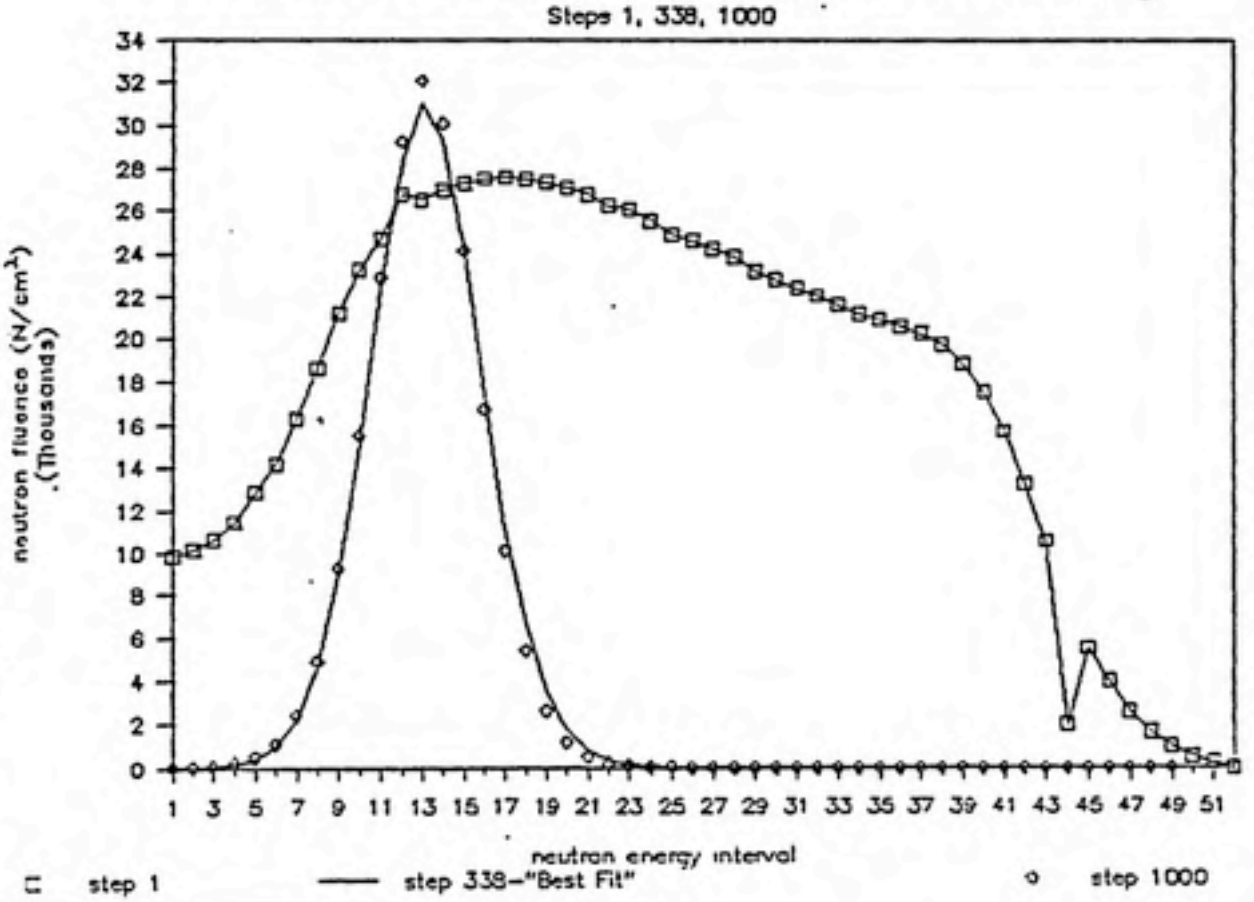

Table 4 PuBe Data, Log-Log Smoothing Alone (step 580)

poly covering	observed counts	σ	2σ range	predicted counts	% deviation (O-P)/O
3"	642	25.3	591.3-692.7	1216.1	89.4
5"	1088	33.0	1022-1154	891.2	18.1
8"	1497	38.7	1420-1574	291.8	80.5
12"	1214	34.8	1144-1284	49.3	95.9

Table 5 PuBe Data, Iteration Alone (step 1500)

poly covering	observed counts	σ	2σ range	predicted counts	% deviation (O-P)/O
3"	642	25.3	591.3-692.7	642.2	0.031
5"	1088	33.0	1022-1154	1087.6	0.036
8"	1497	38.7	1420-1574	1497.7	0.047
12"	1214	34.8	1144-1284	1213.5	0.041

Table 6 PuBe Data, Iteration-Smoothing (step 1500)

poly covering	observed counts	σ	2σ range	predicted counts	% deviation (O-P)/O
3"	642	25.3	591.3-692.7	628.6	2.1
5"	1088	33.0	1022-1154	1126.6	3.5
8"	1497	38.7	1420-1574	1474.0	1.5
12"	1214	34.8	1144-1284	1077.1	11.3

Table 7 Accelerator Data, log-Log Smoothing Alone (step 875)

poly covering	observed counts	σ	2σ range	predicted counts	% deviation (O-P)/O
Bare	5875	76.6	5722-6028	19467.7	231.0
3"	63000	251.0	62448-63500	60937.5	3.27
5"	42725	206.7	41138-	44120.7	3.27
8"	7900	89.9	7722-8078	14568.6	84.4
12"	675	26.0	623-727	2565.4	280

Table 8 Accelerator Data, Iteration Alone (step 1500)

poly covering	observed counts	σ	2σ range	predicted counts	% deviation (O-P)/O
Bare	5875	76.6	5722-6028	9000.6	53.2
3"	63000	251.0	62448-63500	60717.8	3.6
5"	42725	206.7	41138-	43498.0	1.8
8"	7900	89.9	7722-8078	13394.8	69.6
12"	675	26.0	623-727	2161.7	220.0

Table 9 Accelerator Data, Iteration- Smoothing (step 338)

poly covering	observed counts	σ	2σ range	predicted counts	% deviation (O-P)/O
Bare	5875	76.6	5722-6028	8848.8	50.6
3"	63000	251.0	62448-63500	58753.3	6.7
5"	42725	206.7	41138-	42426.7	0.7
8"	7900	89.9	7722-8078	13170.0	66.7
12"	675	26.0	623-727	2119.2	213.0

of predicted counts (P array) for the PuBe source data and the accelerator data.

Referring to table 1, it is quickly noted that the width of the energy intervals, ie, 0-1, 1-2, etc., is not consistent throughout the range of neutron energies presented. The energy intervals continually widen going from interval number 1 to 52. For this reason, the graphical shapes of the "best fit" neutron spectra as presented in figures 5 and 8 are misleading. The visual features on these graphs are more a function of neutron energy interval width than actual neutron fluence at any given energy. The reader may refer to figures 12 and 13 (probability density distributions) of the respective "best fit" spectra normalized to energy interval width. Here the fluence obtained for any interval was divided by the width of that interval in eV. To give the plots still more meaning, the respective spectra were plotted against a consistent energy scale (figures 14 and 15).

These plots were developed by normalizing fluences obtained in figures 12 and 13 respectively in particular energy intervals of interest and plotting them against a common normalized scale. Figure 16 shows the PuBe neutron spectrum determined by Anderson and Neff using a fast neutron spectrometer, employing pulse shape discrimination, and utilizing a single stillbene crystal[12]. Figure 17 shows figure 14 superimposed with the Anderson and Neff spectrum. The Anderson and Neff spectrum (in figure 17) has been scaled to yield the same

Figure 12.

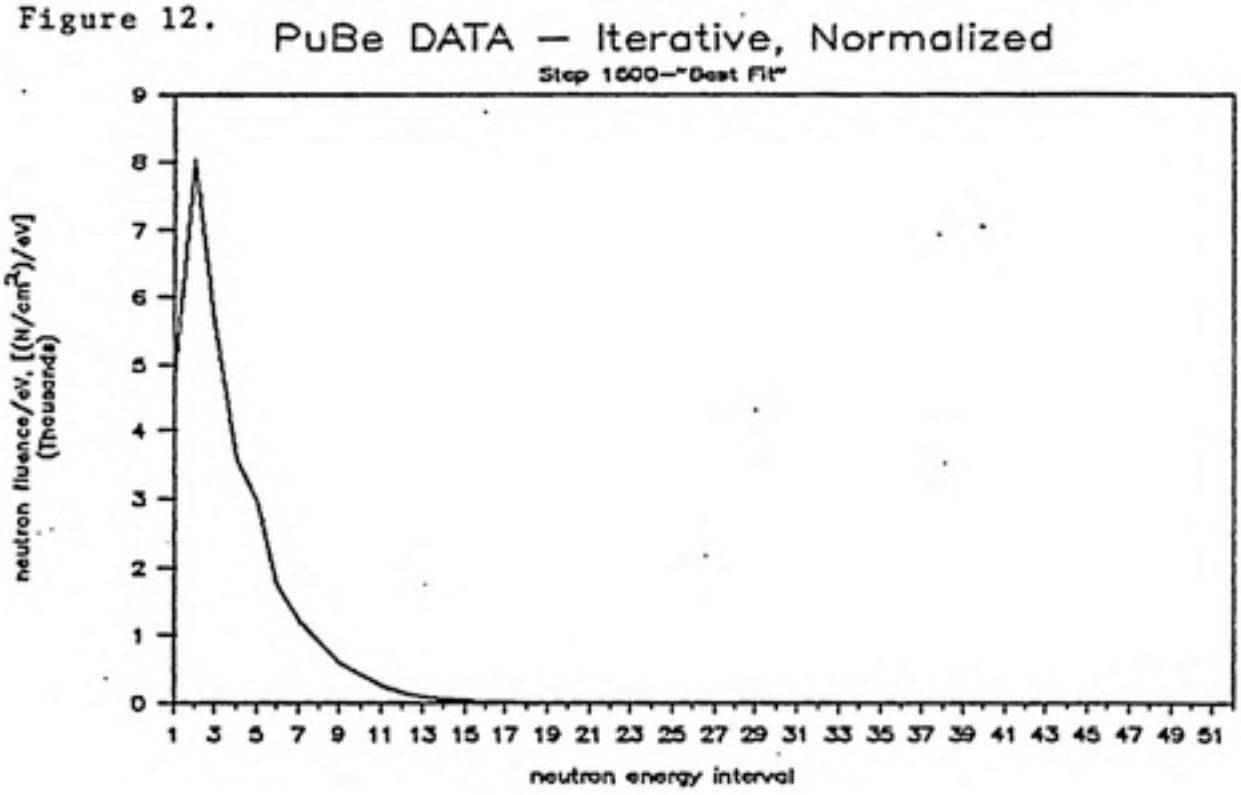

Figure 13.

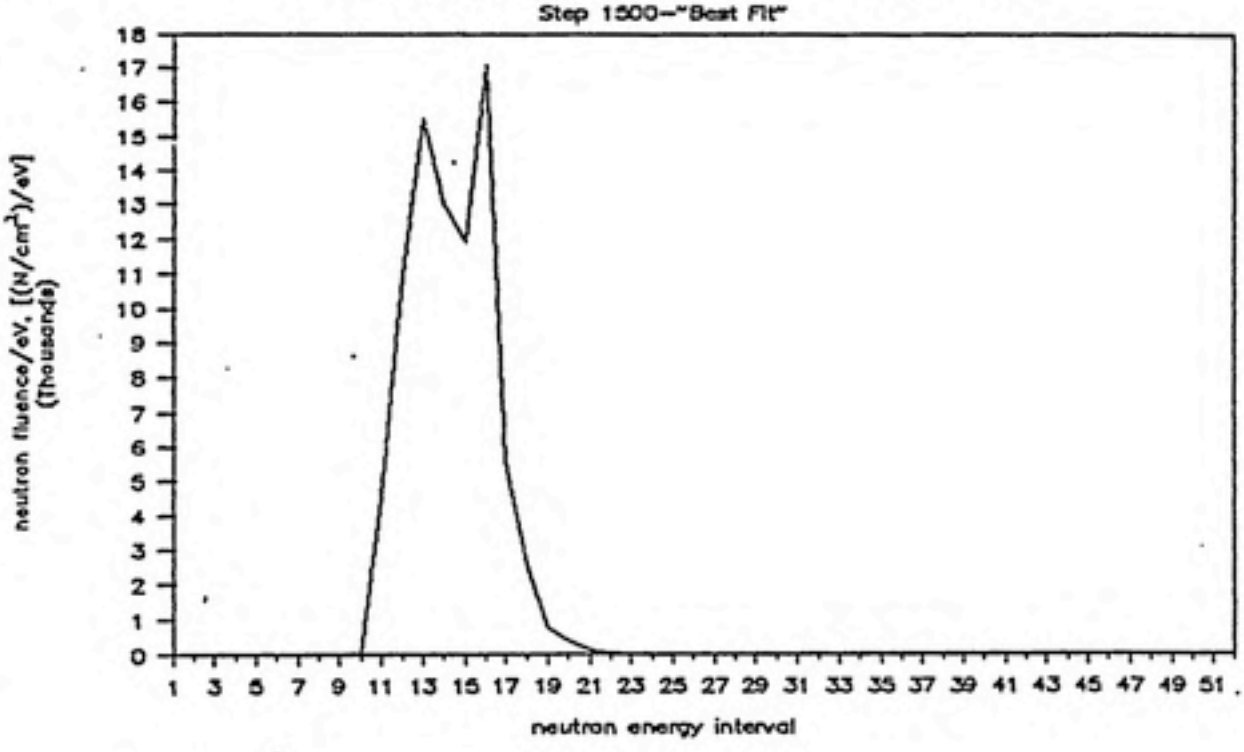

Figure 14

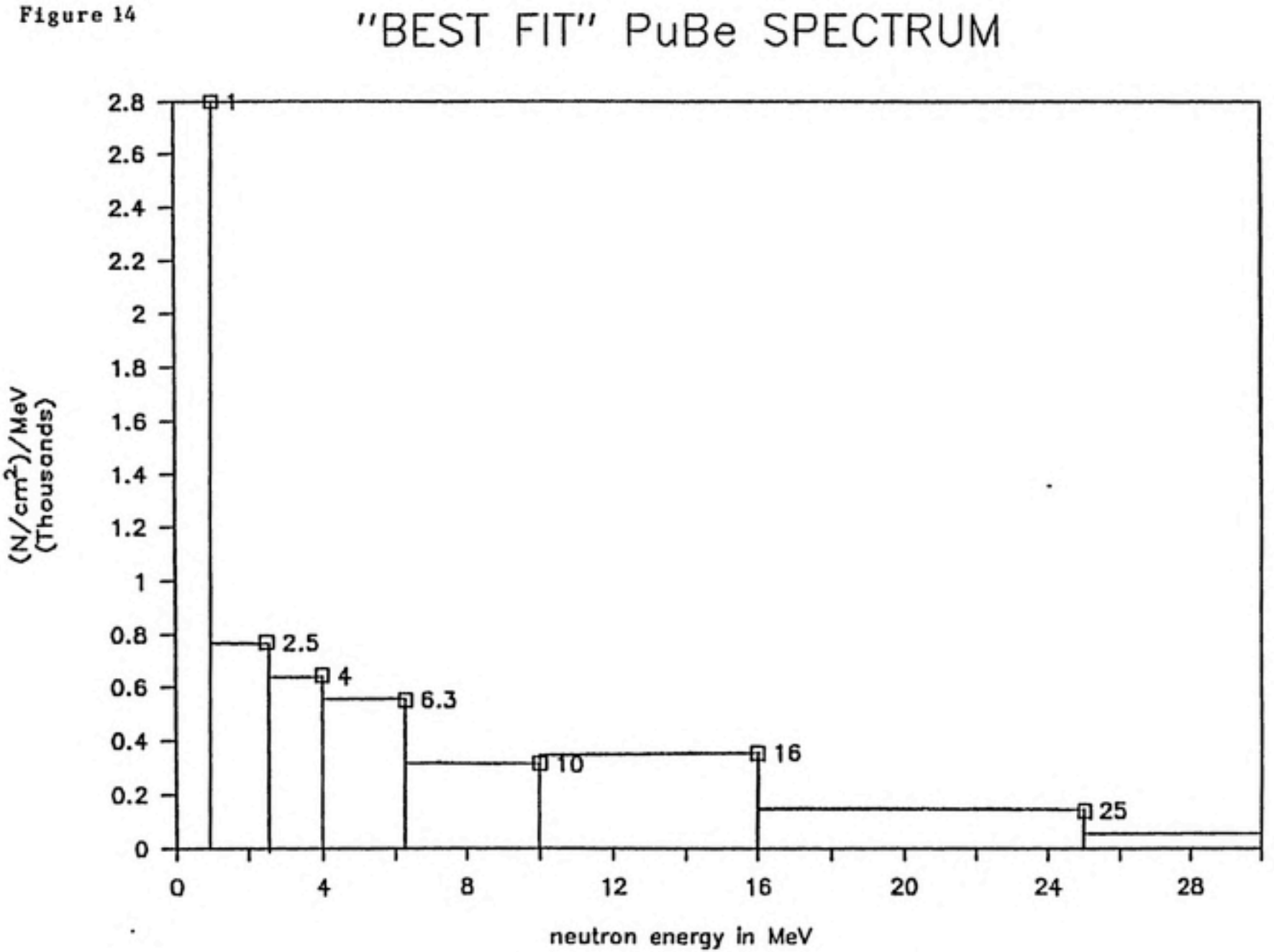
"BEST FIT" PuBe SPECTRUM
(N/cm²)/MeV
(Thousands)
2.8
2.6
2.4
2.2
2
1.8
1.6
1.4
1.2
1
0.8
0.6
0.4
0.2
0
1
2.5
4
6.3
10
16
25
0
4
8
12
16
20
24
28
neutron energy in MeV

Figure 15.

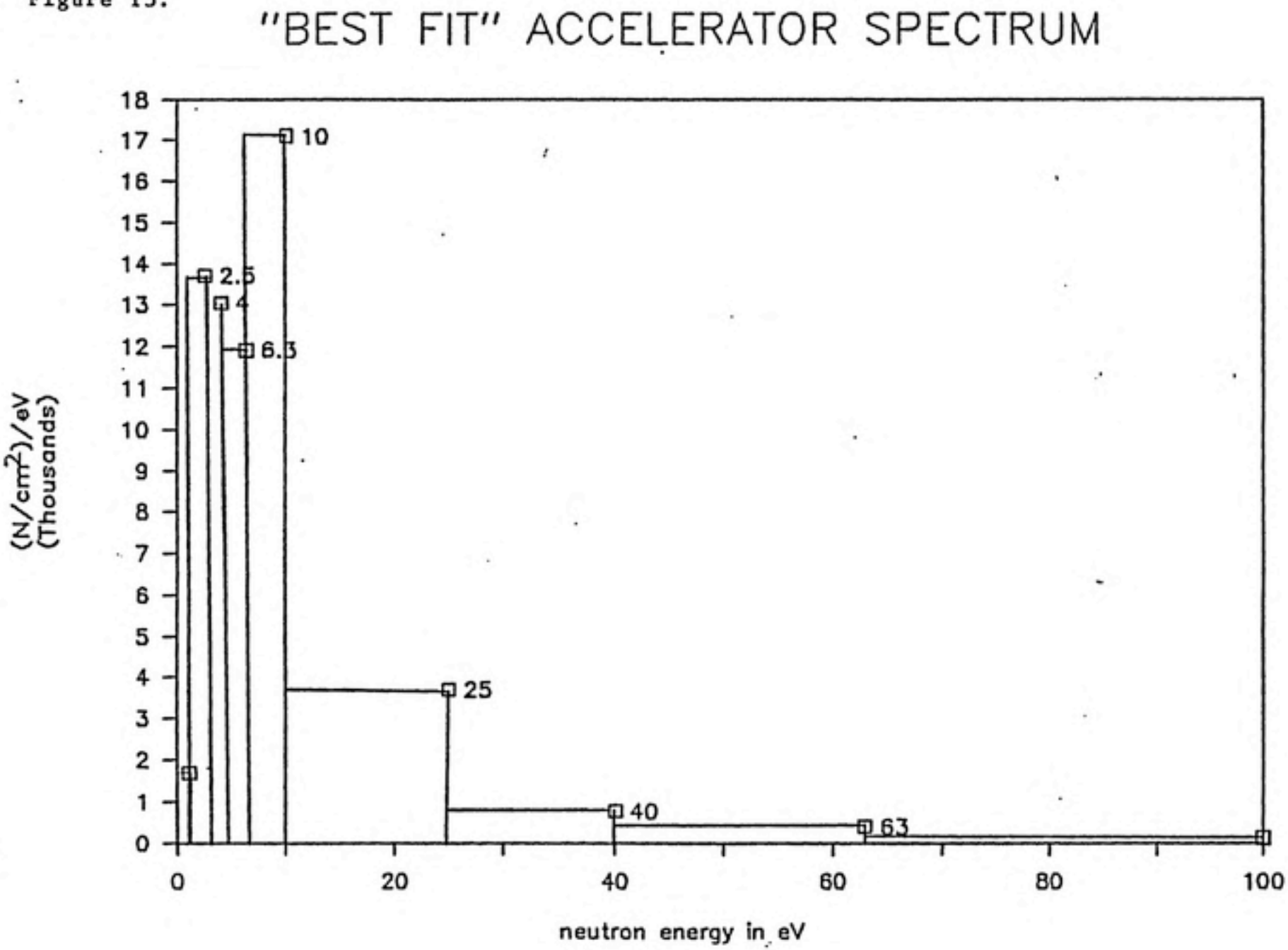
"BEST FIT" ACCELERATOR SPECTRUM
(N/cm²)/eV
(Thousands)
18
17
16
15
14
13
12
11
10
9
8
7
6
5
4
3
2
1
0
10
2.5
4
6.3
25
40
63
0
20
40
60
80
100
neutron energy in eV

Figure 16.

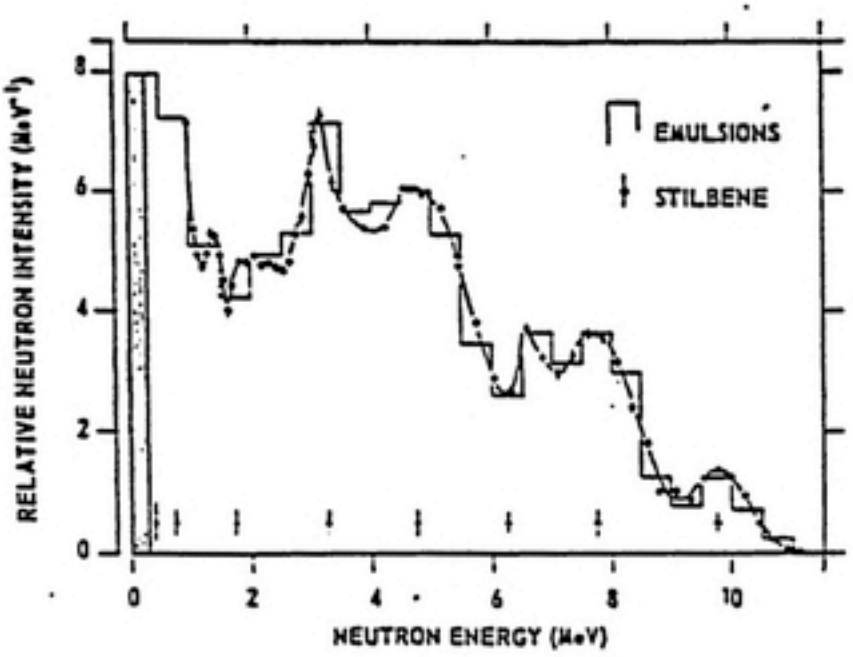

Neutron energy spectrum of Pu–Be source M-591 containing 80 g of Pu. (12)

Figure 17

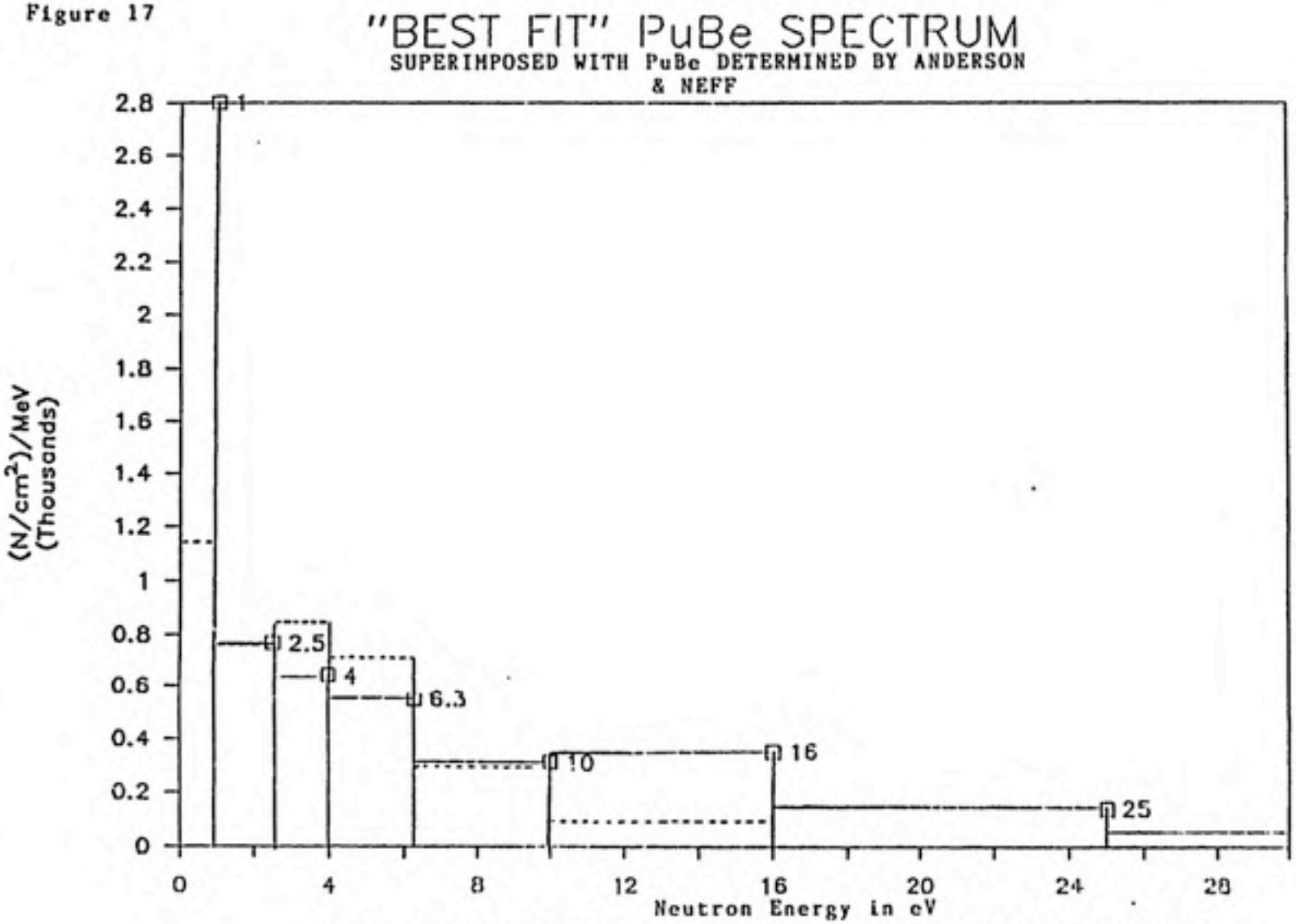

The Anderson and Neff spectrum is broken into energy intervals to correspond to this study. The relative intensities in these energy intervals were calculated from Anderson and Neff data and the absolute intensity in each interval calculated by setting the absolute intensity in the 1.0 - 2.5 MeV interval equal to that obtained in the present study.

——— Present study ----- Anderson & Neff

total number of neutrons as computed by the computer codes used in this research as a means of comparison. The significance of these plots will be discussed in later sections of this paper.

6. CONCLUSIONS

Through a review of the data presented, it is evident that the log-log smoothing routine operating in the computer program alone provides the worst solution to the matrix equation of the three program trials. This conclusion can be arrived at by looking at the % deviation columns in tables 4 and 7. In other words, the smoothing routine yields a solution spectrum with large residual errors compared to other routines.

There is a difference in the spectral shapes produced by the smoothing alone and iterative alone routines when comparing spectra at their respective "best fit" steps (i.e. the iteration that produces the lowest residual error). This can be explained by the fact that each time through the recursion loop, the log-log smoothing routine shapes the curve in a logarithmic fashion (see figures 6 and 9). The smoothing routine then, is merely logarithymicaly altering the previous X array during each iteration. The "best fit" spectrum from the smoothing routine alone has no obvious physical meaning but it is interesting to note how close this simple method actually came to solving the matrix equation (see the % deviation columns in tables 4 and 7).

In computer program trials with both sets of data, the neutron spectra produced with the iterative alone and iterative-smoothing techniques are very similar. The iterative-smoothing trial "best fit" spectrum appears as a smoothed version of the iterative "best fit" spectrum.

It is interesting to note that for both PuBe and accelerator data the iterative alone routine solution was better than the iterative-smoothing solution, this conclusion being arrived at by looking at residuals for the "best fit" steps (table 10). The log-log smoothing routine was added to give more realistic results, as a smooth (continuous) shape was expected, and to help in the approximation of the solution array. It would seem, however, that the smoothing routine may prove more a liability than an asset in solving the matrix equations, at least as far as residual errors are concerned. The smoothed spectrum is, however, more physically realistic.

The iterative routine, operating in the computer program with the smoothing routine disabled, leads to somewhat conflicting observations. Looking at the PuBe data at step 1500 ("best fit") in table 5 and figure 7 it is noted that the routine is solving the matrix equation excellently (with very small % deviation). Whether or not it is solving for the actual neutron spectrum is another matter, since many solutions may be available. As a test of the ability of the code to reproduce data obtained by more precise measurement methods, the calculated PuBe spectrum in it's normalized form, as shown in figure 14, is compared to the general shape to the

Table 10 Residuals (array AL) Incurred at "Best Fit" Steps

Program Trial	Residuals
PuBe-Smoothing Alone	3177352.0.
PuBe-Iteration Alone	0.0996
PuBe-Iteration-Smoothing	20935.6
Accelerator-Iteration Alone	47978479.2
Accelerator-Iteration-Smoothing	56835457.4

PuBe spectrum as reported by Anderson and Neff[12] in the energy regions of dosimetric significance (figure 16). The computed spectrum, however, extends to energy levels far in excess of the spectrum reported by Anderson and Neff and appears to be quite unreasonable with respect to those higher energies. In this regard it may be concluded that the current versions of the computer routines tend to "flatten" the spectrum, pushing the spectrum to higher than reasonable energies.

The iterative routine operating alone solves the matrix equation for both the PuBe data and the accelerator data better than the other methods, considering the amount of residual (table 10) and the % deviation (tables 3 and 6). Also, it solves the PuBe matrix equation nearly exactly while leaving much to be desired with the accelerator matrix equation. This can be seen by comparing the % deviation in tables 5 and 8. Still, the accelerator spectrum (figure 15) would appear to be qualitatively reasonable given what is known about the moderation of neutrons in the head and walls of linear accelerator installations. The accelerator spectrum as shown in figure 15 occurs almost wholly below 100 eV. This makes good intuitive sense as the mean energy of the primary spectrum emanating from the accelerator head is generally considered to be about 1 MeV. It is certainly reasonable to expect the neutrons to be in the slow to thermal energy range by the time they reach the Bonner sphere positioned as shown in figure 5. This is because the great majority of neutrons

before reaching the detector/Bonner sphere combination have undergone many interactions in the concrete walls of the therapy room and have lost energy through elastic collisions with hydrogen in the concrete. Still, some higher energy neutrons would have been expected, and their absence indicates a potential problem with the method.

A possible problem associated with the accelerator "best fit" spectra as presented in figures 10 and 11 is that there is no low energy tail. This tail would be expected to be present and quite prominent due to the low energy neutron fluence which is thought to be quite uniform in the treatment room. As noted for the PuBe source, the computer routines tend to flatten the spectrum, also pushing the spectrum to higher energies. This would not, however, account for the complete removal of the low energy tail. Keeping this in mind, it is easy to understand why the spectra as presented in figures 13 and 15 are preferred. These figures, particularly figure 15, give a more understandable representation of the spectrum including the low energy tail.

Note the extended high energy tail seen in figures 14 and 15 for the PuBe source and accelerator and the over estimation (by the computer program) of the 12" detector/sphere combination seen in tables 8 and 9. A possible reason for the over estimation of counts in the largest sphere size (for the accelerator data) is that reported response coefficients in the A matrix are included for neutron energy intervals in excess of peak photon, and, therefore, peak neutron energies.

These energy intervals are found in steps 48 through 52 (table 1). The iterative routine may try to fit neutron fluences into these energy intervals, thereby overestimating the count of the 12" poly sphere detector (which is the most responsive detector to neutrons of these energies) thereby extending the computed spectrum to energy levels higher than are actually occurring. The iteration routine then may effectively take some low energy fluences and push them into higher energy levels. This effect of spectrum extension caused by the presence of response coefficients in excess of peak neutron energies in the matrix equation may also be occurring in the computer runs made on PuBe data, although no over estimation of the 12" detector/sphere size is seen.

In order to test the possibility that inclusion of high energy response coefficients might be moving neutrons from low to high energies, the codes were run with and without response coefficients at high energies. The effect of spectrum extension or shifting mentioned above would probably be more pronounced for the PuBe data than the accelerator data if this is in fact occurring. This is because the PuBe spectrum naturally extends to a much higher energy range than the scattered fluence from the accelerator. A test run was made on both sets of data with all response coefficients for neutron energy intervals higher than the realm of possibility omitted (higher than the upper energies of the particular neutron source). A test run of the computer program on the accelerator data with response coefficients for neutron energy

intervals 48 - 52 omitted produced exactly the same spectrum with the same residual at the "best fit" step as computer runs made with those intervals included. Trial runs made on the PuBe data with the response coefficients for neutron energies in excess of 16 MeV deleted failed to converge onto a solution. Clearly, response coefficients cannot simply be omitted as tried here. Future studies might focus on a method for dealing with the problem of unreasonably high energies in the response matrix.

It is clear that the neutron counting system presented in this paper gives reasonably good data and performs reliably, in the sense that residual errors between Y and AX can be made quite small. What is not so clear is whether the computer program gives reasonable shapes to the neutron spectra. The relatively good qualitative fit of figure 14 (the normalized "best fit" PuBe spectrum) to the PuBe spectrum reported by Anderson and Neff (figure 16) in the region of dosimetric interest shows that the unfolding method presented at least has some merit and bears further investigation. Looking at the computed accelerator spectrum again (from the last section) we may note that the counts for some detector/sphere combinations predicted using the iterative only routine fell far from the actual counts in those detectors. This, in combination with the high residuals, would lead us to believe that this best fit spectrum, in fact, fits rather poorly. One must bear in mind, however, two important points. The first is that the residuals are the squared difference between the

observed and predicted counts, and the second is that the accelerator "best fit" spectrum predicts counts in four detector/sphere combinations quite well. If the spectrum reproduces the measurement data for four out of five independent linear equations, the spectrum cannot be too far from being a reasonable approximation.

Assumed losses of fluences in the low energy range and over-estimations in the high energy range remain significant features. Table 11 displays neutron quality factors relative to fluence and energy [13]. Loss of neutron fluences in the near-thermal energy range is not that critical, as this is where quality factors are lowest. Over estimations of the high energy range would only lead to more conservative calculations, as this is where quality factors are highest. For the most part, however, neutron fluences per unit energy above 100 eV in the calculated accelerator spectrum are extremely small, and are nearly non-existent above 250 eV. This could have important implications in shielding calculations, which require information on the higher energy neutrons.

In order to obtain better estimates of neutron spectra in the future using techniques similar to the one presented in this paper, several points may be raised. First, the presence of response coefficients above the range of expected neutron energies warrants further investigation. Another is that other smoothing routines may be tried, log-log smoothing perhaps not being the best approach. An arithmatic (linear-

Table 11
Neutron quality factors at various energies

Neutron Energy (MeV)	Quality Factor	Relative $N/cm^2/s$
thermal	3	67.0
0.0001	2	50.0
0.005	2.5	57.0
0.02	5	28.0
0.1	8	8.0
0.5	10	3.0
1.0	10.5	1.8
2.5	8	2.0
5.0	7	1.8
7.5	7	1.7
10	6.5	1.7
10-30		1.0

linear) approach is one possibility. Lastly it may be possible to give the computer program a better initial starting spectrum. This a priori spectrum would have to be one of a shape which is highly expected from past measurements or theoretical considerations. Other authors have suggested this approach and have used it[3][5]. The value of this approach is questionable, however, since it is not clear what spectrum should be assumed at the start and how that choice affects the results. A possible advantage to such an approach, however, is that it might be more efficient in terms of computer time, as fewer recursion loops would be necessary (assuming you chose the right initial spectrum).

The unfolding process as presented in this paper seems to give qualitatively reasonable results for both PuBe and accelerator data. With further work aimed at resolving the problems associated with spectrum shifting and choice of initial spectrum, this process may be used in conjunction with existing and future shielding calculations to provide adequate barriers to neutron contamination in linear accelerator radiation therapy rooms.

APPENDIX A

The Computer Program

(as modified to handle the accelerator data)

```
C    data input section and echo out
1 IMPLICIT REAL*8 (A-H), INTEGER (I-N)
2 REAL*8
3 A(5,52),X(52),Y(5),B(52,52),AT(52,5),W(52),Z(52),R(5),
4 P(52),D(52,52),AL(1000)
5     DO 20, I=1,5
6      READ(5,FMT=10)(A(I,J),J=1,52)
7      READ(5,FMT=30) Y(I)
8 30    FORMAT(F7.1)
9      WRITE(6,FMT=15)(A(I,J),J=1,52)
10 15    FORMAT(1X, 9F7.4)
11 10    FORMAT(9F7.4)
12 20   CONTINUE
13    WRITE(6, FMT=40)(Y(I),I=1,5)
14 40   FORMAT(5F10.4)
C   transpose of A matrix
15    DO 50, I=1,52
16    DO 50, J=1,5
17     AT(I,J)=A(J,I)
18 50   CONTINUE
C   building of initial spectrum
19    DO 60, I=1,52
20     WBT=0
21     DO 70, J=1,5
22      WBS=AT(I,J)*Y(J)
23      WBT=WBT+WBS
24 70    CONTINUE
25     WB(I)=WBT
26 60   CONTINUE
27    DO 80, K=1,52
28     DO 90 I=1,52
29      BT=0
30      DO 100, J=1,5
31       BS=AT(I,J)*A(J,K)
32       BT=BT+BS
33 100     CONTINUE
34       B(I,K)=BT
35 90    CONTINUE
36 80   CONTINUE
37    N=0
38    DO 110, I=1,52
39     X(I)=WB(I)
40 110  CONTINUE
C   beginning of recursion loop
41    DO 500, N=1,2500
C   smoothing of each spectrum in loop
42    DO 120, J=2,52
43      IF (X(J-1) .LE. 1.0) THEN
44      X(J-1)=1.1
```

```
45      END IF
46      IF (X(J+1) .LE. 1.0) THEN
47      X(J+1)=1.1
48      END IF
49      IF(X(J) .LE. 1.0) THEN
50      X(J) =1.1
51      END IF
52     X(J)=DEXP(DEXP((DLOG(DLOG(X(J-1)))+4*DLOG(DLOG(X(J)))+
53       DLOG(DLOG(X(J+1))))/6))
54 120  CONTINUE
C  printing of various spectra
55    IF (N .EQ. 1.0) THEN
56    PRINT*, 'N =',N
57     DO 121, I=1,52
58     PRINT*, 'X',I,'=',X(I)
59 121  CONTINUE
60     END IF
61    IF (N .EQ. 500) THEN
62    PRINT*, 'N =',N
63 DO 122, I=1,52
64     PRINT*, 'X',I,'=',X(I)
65 122  CONTINUE
66    END IF
67    IF (N .EQ. 875) THEN
68    PRINT*, 'N =',N
69     DO 123, I=1,52
70     PRINT*, 'X',I,'=',X(I)
71 123  CONTINUE
72    END IF
73    IF (N .EQ. 1000) THEN
74    PRINT*, 'N =',N
75     DO 124, I=1,52
76     PRINT*, 'X',I,'=',X(I)
77 124  CONTINUE
78    END IF
79    IF (N .EQ. 1500) THEN
80    PRINT*, 'N =',N
81     DO 125, I=1,52
82     PRINT*, 'X',I,'=',X(I)
83 125  CONTINUE
84    END IF
C  calculation of predicted counts in bonner spheres
85    DO 130, K=1,5
86     P(K)=0
87     DO 140, M=1,52
88      Z(M)=0
89      Z(M)=A(K,M)*X(M)
90      P(K)=Z(M)+P(K)
91 140    CONTINUE
C  calculation of residuals each bonner sphere
92     R(K)=(Y(K)-P(K))**2
93 130  CONTINUE
C  printing of predicted counts
94    IF (N .EQ. 875) THEN
```

```
95    PRINT*, 'N =',N
96    DO 145, K=1,5
97     PRINT*, 'P(K)',K,'=',P(K)
98 145  CONTINUE
99    END IF
C  calculation of total residual for loop
100   AL(N)=0
101   DO 150, K=1,5
102    AL(N)=AL(N)+R(K)
103 150  CONTINUE
C  calculation of new spectrum (X array)
104   DO 160, I=1,52
105    WVT=0
106    DO 170, J=1,52
107     WVS=B(I,J)*X(J)
108     WVT=WVT+WVS
109 170   CONTINUE
110    WV(I)=WVT
111 160  CONTINUE
112   DO 180, I=1,52
113    D(I,I)=X(I)/WV(I)
114 180  CONTINUE
115   DO 190, I=1,52
116    X(I)=D(I,I)*WB(I)
117 190  CONTINUE
118 500  CONTINUE
C  printing of final X array
119      PRINT*,'X'
120   DO 200, I=1,52
121    PRINT*,'X',I,`=`,X(I)
122 200  CONTINUE
C  printing of residuals
123   PRINT*, '   '
124   PRINT*, 'AL',
125   DO 550, N=1,2500
126    PRINT*, 'AL`,N,`=`,AL(N)
127 550  CONTINUE
128      RETURN
129   END
```

References

1. R.L. Bramblett, R.I. Ewing, T.W.Bonner, Nuclear Instruments and Methods, Vol. 9, pp. 1-12 (1960).

2. G.F. Knoll, Radiation Detection and Measurement, John Wiley and Sons, New York, (1979) pp. 551-561.

3. G.L. Watkins and G.R. Holeman, Health Physics, Vol. 15, PP.535-539.

4. K. O'Brien, R. Sanna, J. McLaughlin, First Symposium on Accelerator Radiation Dosimetery and Experience, USAEC-CONF-651109, p.346 (1965).

5. K.A. Lowery, T.L. Johnson, Health Physics, Vol. 47, pp.587-593 (1984).

6. L. W. Brackenbush, R. I. Scherpelz Computer Applications in Health Physics, Proceedings of the 17th Midyear Topical Symposium of the Health Physics Society, (1984).

7. P.D. LaRiviere, Medical Physics, Vol. 12(6), pp.806-809 (1985).

8. R.C. McCall, W.P. Swanson, NBS Special Report 554, p. 75 (1979).

9. E.J. Axton, A.G. Bardell, NBS Special Report 554, p.109 (1979).

10. NCRP Report No. 79 pp. 1-57

11. H. W. Patterson, R. Wallace, Lawrence Berkeley Lab, Berkeley, CA, Report No. UCRL-8359 (1958).

12. M.E. Anderson, R.A. Neff, Nuclear Instrumentation and Methods, 99(1972) pp. 231-235.

13. M.E. Anderson, W.H. Bond, Jr., Nuclear Physics, 43(1963) p. 330.